Agronomic performance and GHG emission profile of rice and koronivia grass cultivated in a tropical environment

Fredrik Mikael Larsson

Degree project/Independent project • 60 credits
Swedish University of Agricultural Sciences, SLU
Department of Crop Production Ecology (VPE)
Agriculture Programme – Soil and Plant Sciences
Place of publication Uppsala 2025

Agronomic performance and GHG emission profile of rice and koronivia grass cultivated in a tropical environment

Agronomisk utveckling och växthusgasemissioner från ris och koroniviagräs odlat i tropisk miljö.

Fredrik Mikael larsson

Supervisor:	**Marcos Lana, Swedish University of Agricultural Sciences, Department of Crop Production Ecology; Agricultural Cropping Systems**
Assistant supervisor:	Miguel Antonio Romero Sanchez, CIAT Colombia and SLU
Examiner:	Ingrid Öborn, Swedish University of Agricultural Sciences, Department of Crop Production Ecology; Agricultural Cropping Systems

Credits:	60 credits
Level:	Second cycle, A2E
Course title:	Master Thesis in Biology
Course code:	EX0900
Programme/education:	Agriculture Programme – Soil and Plant Sciences
Course coordinating dept:	Department of Aquatic Sciences and Assessment
Place of publication:	Uppsala
Year of publication:	2025

| **Keywords:** | rice, koronivia grass greenhouse gas emissions |

Swedish University of Agricultural Sciences
Faculty of Natural Resources and Agricultural Sciences
Department of Crop Production Ecology (VPE)

Abstract

Managed forage grazing alongside flood-irrigated rice cultivation is recognized as a significant contributor to GHG emissions into the atmosphere. Forage grazing releases large amounts of nitrous oxide emissions, which can be reduced using species such as koronivia grass (*Brachiaria humidicola*), a forage grass known for its biological nitrification inhibition capacity through the root exudate called brachialactone. Rice cultivation releases large amounts of methane into the atmosphere, which is why greenhouse gas emissions from flood-irrigated rice paddies have been extensively studied in Asia; however, few studies have been conducted in Latin America, including Colombia, highlighting the need to understand the topic in this region better.

Rice cultivation and forage grazing are two of Colombia's most important agricultural activities; therefore, assessing GHG emissions from these activities is of utmost importance since no GHG emission factors are available for these two cropping systems under Colombian conditions.

This study aims to provide insight into the key characteristics of greenhouse gas emissions and yield-related components of different rice and koronivia grass cultivars in Colombia through a field trial of two rice and two koronivia grass cultivars, contributing to a better understanding of the environmental effects of cultivation in tropical areas of South America. To achieve this goal, biomass and yield components were evaluated, along with CH_4 and N_2O emissions and emission factors, with a specific focus on differences in root biomass between cultivars.

The rice and koronivia grass field trials were conducted at the CIAT Research Center in Colombia, where soil samples were collected before the trial started. The experimental layout consisted of a randomized block design with three replications of each rice and koronivia grass cultivar. Within each replication, three closed static chambers were placed and used as subsamples, with gas concentrations quantified using gas chromatography. An automatic weather station was used to gather environmental data during the sampling period.

Rice cultivar HL23 had a higher grain yield and greater daily methane emissions during the beginning of the sampling period. Meanwhile, cultivar FE60 displayed a larger variance in daily CH_4 emissions from flowering to the end of the sampling period. This study presents the first reported field-emitted methane emissions from a koronivia grass field experiment. The koronivia grass cultivar CI67 displayed a significantly higher variance in daily CH_4 emissions during the beginning of the sampling period, and a trend was observed where cultivar CI67 had higher cumulative CH_4 emissions. This study also provides insight into the key characteristics of CH_4 and N_2O emissions and yield-related components of different rice and koronivia grass cultivars.

Keywords: rice, koronivia grass, greenhouse gas emissions

Table of contents

List of tables

List of figures

Abbreviations

CI67	Koronivia grass cultivar (CIAT 679)
BH08	Koronivia grass cultivar (BH08-1149)
FE60	Rice cultivar (Fedearroz 60)
HL23	Rice cultivar (HL 23057)
DAS	Days after sowing
pGWP	Partial global warming potential
YpGWP	Yield -scaled partial global warming potential
PCA	Principal component analysis
GHG	Greenhouse gas
PVC	Polyvinyl chloride
FID	Flame ionization detector
ECD	Electron capture detector
GLMER	Generalized linear mixed-effects model

1. Introduction

Nitrous oxide (N_2O) is the world's third most important greenhouse gas with a lifetime of 100 – 150 years (Albanito et al. 2017), with a global warming potential 298 times stronger than CO_2. Production of N_2O occurs naturally through microbial processes in soil through the process of nitrification and denitrification. In agriculture the main reason for N_2O emissions comes from the application of organic and inorganic fertilizer during periods when the plants can not take up the fertilizer amount (Wang et al. 2021). Thanks to agricultural fertilization practices with increased organic and synthetic nitrogen, the nitrogen fertilizer used in agriculture have increased from 4 to 120 ± 10 % TgN yr^{-1} globally since the 1950s. While it increases yield, the nitrogen use efficiency of 20-30 % is converted into food, and results in the most significant source of increased nitrogen loss, through N_2O emissions, NH_3 volatilization, and other reactive nitrogen forms (Albanito et al. 2017). Other factors affecting N_2O emissions include available soil carbon, readily available for microorganisms, and soil water content, where higher water content increases N_2O production. The finer soil texture in heavier soils has higher emissions due to higher water-holding capacity and more anaerobic environments, and higher soil temperature increases N_2O emissions by affecting the growth rate of the microorganisms (Wang et al. 2021). Managed grazing by animals for milk, meat, and fiber production, covers one-quarter of the global land surface area and is the most extensive agricultural activity (Kelliher et al. 2014). Cattle production in Colombia alone presents a land occupation of 37 million ha with 27 million animals nationwide, providing an important source of livelihood and income for many small to large-scale farmers. The cattle production relies on extensive grazing pastures, these pastures are often periodically exposed to overgrazing and sequential pasture degradation due to lack of management and low precipitation during the dry season. In this system, urine and manure are randomly deposited by cattle, resulting in patches with high nitrogen concentration and potentially significant loss due to ammonia and nitrous oxide emissions (Durango Morales et al. 2021a).

The amount of N_2O emission from managed grasslands depends partly on the root length (Abalos et al. 2018) and species used (Simon et al. 2020). The forage grass koronivia grass (*Brachiaria humidicola*) is known for its biological nitrification inhibition capacity through the root exudate named brachialactone, a

cyclic diterpene (Subbarao et al. 2009), which causes a reduction of N_2O emissions when compared to other forage species such as *Eremochloa ophiuroide* and *Panicum maximum* (Simon et al. 2020; Xie et al. 2022), however, koronivia grass is considered a poor quality grass with relatively low crude protein levels and low digestibility (Villegas et al. 2023). It is hypothesized by Simon et al. (2020) that longer roots and higher root biomass density may lead to lower levels of N_2O produced compared to cultivars with shorter root lengths and lower root biomass density contributed by higher root density, creating a more extensive distribution of nitrification inhibiting root exudates in along with higher water uptake, resulting in the reduction of N_2O production.

Methane (CH_4) is one of the greenhouse gases with the highest effect on global warming, with a global warming potential 23 times higher than CO_2 in a time horizon of 100 years. The atmospheric abundance of methane has increased by about 2.5 compared to the pre-industrial era and is estimated to cause 15-20 % of anthropogenic atmospheric radiation forcing (Zou et al. 2005). CH_4 appears and is produced in anaerobic environments devoid of oxygen; the production is driven by organic material breakdown by different groups of anaerobic microorganisms, including hydrolytic, fermenting, homo-acetogenic, syntrophic, and methanogenic (Ma et al. 2009).

Irrigated rice paddies cover an area of roughly 80 million ha and account for about 75 % of the total world production of rice (Camargo et al. 2018), the cultivation is recognized as a significant contributor of CH_4 emissions to the atmosphere and stands for 6-11 % of the global yearly CH_4 emissions from anthropogenic sources (Nikolaisen et al. 2023). Even though studies are abundant regarding CH_4 emissions from rice cultivation (Camargo et al. 2018), the interactive relationship between microbes and rice roots' effect on CH_4 emissions is poorly understood. According to Chen et al. (2019), a bigger root system with bigger biomass causes higher O_2 transport down through the roots, creating a more oxidized root area in the rhizosphere. Oxygen becomes accessible to methanotrophs and increases the breakdown and oxidation of CH_4, potentially reducing CH_4 emissions. Rice is a staple crop for roughly half of the world's population and provides an important energy source and 51.4-69.2 % of the total protein intake for the population of southern Asia, and contributes to 30 % of cereal production globally (Mukamuhirwa 2019), and is expected to increase (Hussain et al. 2015). To satisfy the demands of an increased population there is a need for increased rice production globally (Li et al. 2022), the demand for increased production also highlights the need for more environmentally friendly practices with reduced CH_4 emissions, such as the draining of rice paddies at fertilization events (Loaiza et al. 2024). Studies made in Asia on CH_4 emissions from soil and mitigations are abundant but poorly studied in Latin America, including Colombia, where mechanized seeding is used to a larger extent, indicating the need for a better

understanding of the topic in Latin America (Camargo et al. 2018). The agricultural practices in Colombia depend largely on the region within the country, with important crops such as coffee, grown in mountainous areas (L et al. 2014), while other important agricultural activities such as rice cultivation and forage grazing are more prominent in the savannas and lowlands (Villegas et al. 2023; Loaiza et al. 2024). Therefore, the assessment of the GHG emission profile of methane and nitrous oxide of these activities is of utmost importance, since no GHG emission factors are available for these two cropping systems under Colombian conditions (Durango Morales et al. 2021a).

1.1 Aim

This work aims to evaluate two cultivars of rice (*Oryza sativa)* and koronivia grass (*Brachiaria humidicola)*, respectively, by grain yield (rice), biomass production (koronivia grass), and GHG emissions.

The specific research questions are the following:

1. Do different rice cultivars display differences in grain yield and GHG emission profile (N_2O, CH_4)?
2. Do different rice cultivars display differences in partial global warming potential and yield-scaled partial global warming potential?
3. Do different koronivia grass cultivars display differences in root biomass, above-ground biomass, and the ratio between the two?
4. Do different koronivia grass cultivars display differences in GHG emissions profile, partial global warming potential, and yield-scaled partial global warming potential (methane and nitrous oxide)?

2. Materials and Methods

2.1 Location

The field experiment was conducted during the 2022-2023 season on the campus of the International Centre for Tropical Agriculture (CIAT) in Valle del Cauca, Colombia (3° 30'09"N, 76°21'20"W, 1018 m above mean sea level) (Fig. 1a, b). The region has a tropical dry forest climate with an average annual temperature of 20 ºC and an average annual precipitation of 894mm (Horrocks et al. 2019).

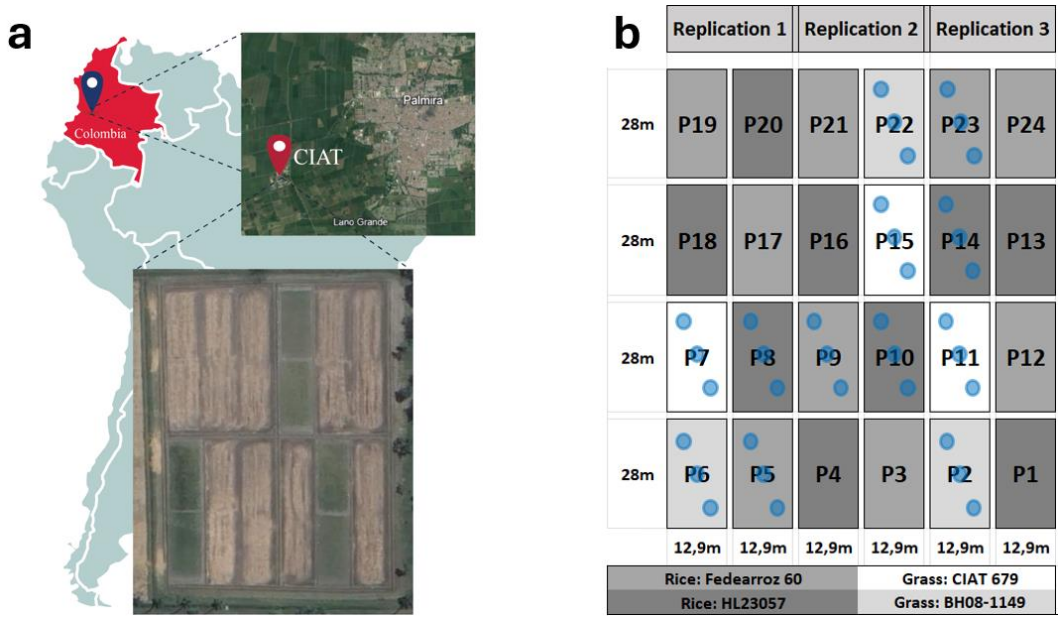

Fig. 1. (a) Map-location of CIAT within Colombia and aerial view of CIAT and experimental area at CIAT (Google Earth. 2023). (b), Layout of field experiment, GHG-emission rice experiment was performed on plots (P) 5, 8, 9, 10, 14, and 23, marked with blue dots. GHG-emission Koronivia grass experiment was performed on plots 2, 6, 7, 11, 15, and 22, marked with blue dots. The remaining plots on site were not included in the GHG-emission experiment but were used for soil analysis, grain, and biomass harvest

2.2 Experimental design

The experiment consisted of randomized block design with three replications (plots) of each cultivar of both rice and koronivia grass (Fig. 1b). Three closed static chambers were placed in each replication and used as subsamples. The weather conditions during the experimental phase are shown in Fig. 2 (a, b, c). All experiments were treated with conventional pesticide and herbicide treatment. The preceding crop was maize for both the rice and forage grass experiments. Regarding cultivars, the genetic material for rice (*Oryza sativa*) cultivars consisted of Fedearroz 60 with long roots and HL23057 (also called CT23057H) with short roots, according to Alvarez, M, F. (2024). The genetic material for the koronivia grass (*Brachiaria humidicola)* consisted of CIAT 679 (long roots) and BH08-1149 (short roots). While the root length was not directly assessed in this experiment, CIAT reports that cultivar HB08-1149 had relatively shorter roots when compared to CIAT 679.

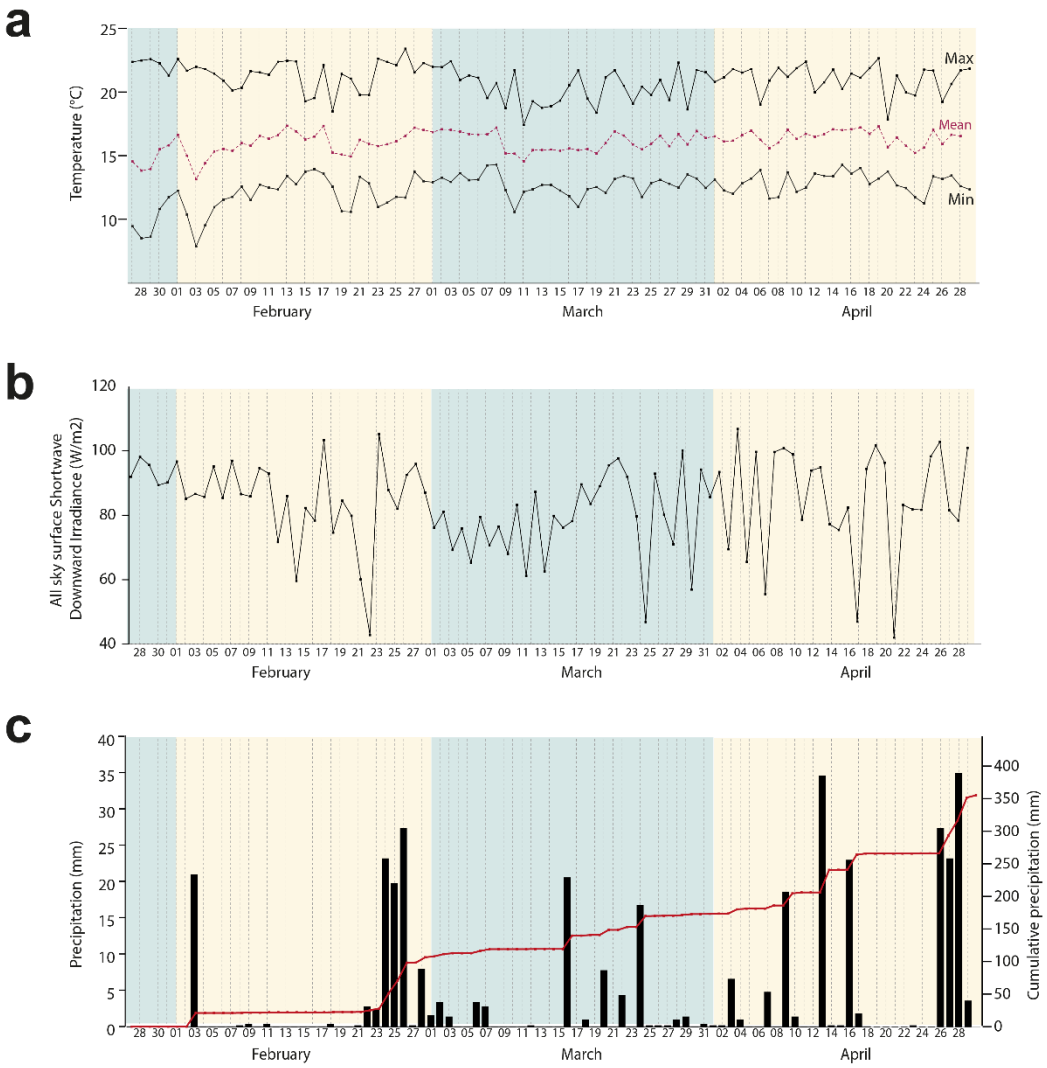

Fig. 2. (a) Maximum, mean and minimum air temperature (ºC), 2m above ground, (b) surface shortwave downward radiation (W m^{-2}) Source: NASA POWER (Westberg, D Stackhouse, P.W et al. 2015), (c) precipitation, and cumulative precipitation (mm)

2.2.1 Rice establishment

The establishment of the rice experiment was done as shown in Fig. 3. The rice experiment started with direct sowing, which was performed on 27th December 2022. The irrigation of the rice experiment began on 31st January and continued until 17th April in a continuous flooding system, aiming at a 6 cm water level. The fertilization of the rice experiment (Fig. 3) showed the total fertilizer amount applied (kg ha^{-1}) and the amount and source of nutrients applied (kg ha^{-1}) in each of the six fertilization applications spanning from December to February.

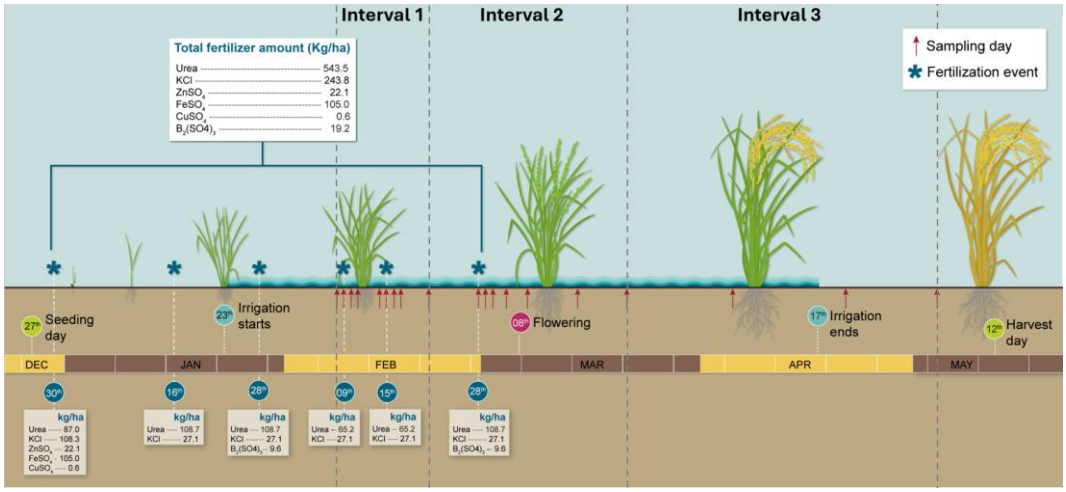

Fig. 3. Rice experiment timeline from December 2022 to May 2023. Show the total fertilizer amount and dates of fertilizer events with the applied fertilizer (star). Date of seeding in field and grain harvest, flowering, period of irrigation with constant water level (6cm), and GHG-emission sampling dates (arrow). Dashed lines display interval separation of the GHG-emission sampling period, Interval one (days 42-55), two (days 62-76), and three (days 83-127)

2.2.2 Forage grass establishment

The establishment of the forage grass experiment was done as shown in Fig. 4, the koronivia grass experiment started with the planting of koronivia grass tillers in pots on 05th November 2022 and then planted in the field on 14th January. The fertilization of the koronovia grass experiment (Fig. 4) showed the total fertilizer amount applied (kg ha^{-1}) and the amount and source of nutrients applied (kg ha^{-1}) in each of the two fertilizer applications (3rd February and 7th March).

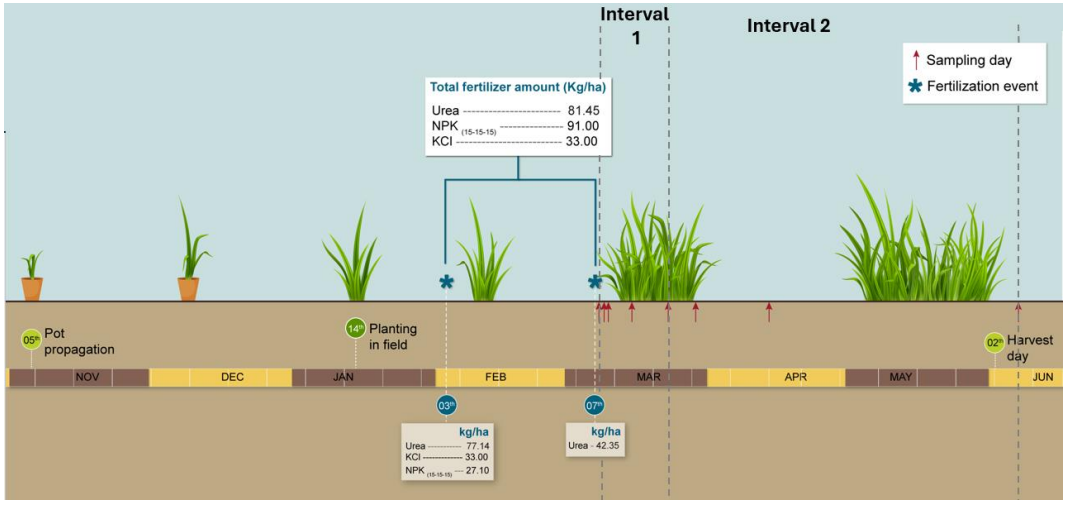

Fig. 4. Timeline of field experiment of koronivia grass. Koronivia-grass experiment timeline from November to June. Show the total fertilizer amount and dates of fertilizer events with the applied fertilizer (star). Date of potting of tillers, planting in field and biomass-harvest, and GHG-emission sampling dates (arrow). Dashed lines display interval separation of the GHG-emission sampling period, Interval one (days 54-61), and interval two (days 69-145)

2.3 Field measurements

2.3.1 Environmental data collection and soil sampling and analysis

An automatic weather station was placed close to the experimental area from 10th February to 12th May 2023. Precipitation (mm) was measured by one rain gauge model ECRN-100, while soil water content and soil temperature (ºC) were measured for each experimental plot in the rice experiment at five-centimeter soil depth by two TEROS 11 soil sensors, with automatic datalogger model ZL6 Basic. Air temperature (ºC), atmospheric pressure (Pa), and absolute air humidity (g m^{-3}) were measured at each sampling event with a handheld weather station. Surface shortwave downward radiation (W m^{-2}) and air temperature in ºC (Max, mean, and min, 2m above ground) between sample events were collected from the NASA-POWER database (Stackhouse et al. 2015), (Fig. 2).

In November 2022, soil samples were collected from the experimental site, including 120 ring samples (from the middle of each plot) for the bulk density analysis, and 120 subsamples (consisting of 9 replications per plot) for chemical characterization and soil organic materials analysis (Fig. 5a, b).

All soil samples were taken at five soil depths (0-5, 5-10, 10-30, 30-60, and 60-100 cm). Soil profile samples covering the whole horizon were collected for soil profiles 0-5 and 5-10 cm; samples from horizons 10-30, 30-60, and 60-100 cm were collected by taking one sample in the middle of the horizon, representing the whole horizon.

a

parameters	units	#samples
bulk density	kg/m3	120
chemical characterization	cmol/kg; g/kg; mg/kg	120
soil organic material	g/kg	120

b

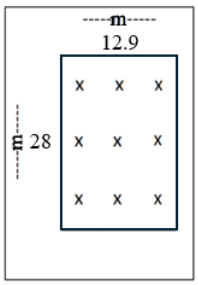

Fig. 5. Soil sample details. (a) soil sample parameters and number (#) of samples, (b) position of the bulk density and subsamples for soil, taken in each plot, for both the koronivia-grass and rice experiment

Soil chemical analysis methods of soil samples were carried out at the CIAT Colombia soil lab and are presented in

Table 1, and the soil chemical and physical measurement mean values for the top 30 cm soil layer are presented in Table 2. The complete table of soil chemical analysis is presented in Table 6 (appendix).

Table 1. Soil chemical analysis methods.

compound	methods	description	reference
pH (Un) C Oxid (g/kg) Al (cmol/kg)	Potentiometry	Measurment of current potential of electrochemical cell under static conditions.	Stork, J.T. (1993)
Zn (mg/kg) Mn (mg/kg) Na (cmol/kg) Ca (cmol/kg) Mg (cmol/kg) K (cmol/kg)	Atomic absorption spectroscopy	detection of soil elements through absorption of characteristic narrow frequency electromagnetic radiation.	Liang (2020)
SOM (g/kg) P-BrayII (mg/kg) Fe (mg/kg) Cu (mg/kg) B (mg/kg) S (mg/kg)	Ultraviolet - Visible spectroscopy	Detects color and intensity from ion levels in solution through light spectroscopy.	Jaffar et al. (2024)

pH: Soil pH, C Oxid: oxidizable carbon, Al: aluminum, Zn: zinc, Mn: manganese, Na: sodium, Ca: calcium, Mg: magnesium, K: potassium, SOM: soil organic material, P-Brayll: plant-available phosphorus, Fe: iron, Cu: copper, B: boron, S: sulfurous. References: (Liang 2020; Jaffar et al. 2024; Stork,J.T. 1993)

Total nitrogen (Tn) represents the nitrogen fraction in the soil, bound in the soil organic matter. The Total nitrogen content was calculated by first calculating the percental total nitrogen, using equation 5. Then, using calculation 6 to calculate Total nitrogen (g kg^{-1} soil), using the density of the soil collected from soil sampling (Table 2).

$$Tn(\%) = (SOM(\%) * 0.05) \quad (5)$$

$$Tn = \frac{(Na\ (\%) * sw) * 10}{sw} \quad (6)$$

Where *SOM (%)* is the percental soil organic matter, which was calculated based on measurements from soil samples (Table 2). The total nitrogen content of organic material was considered to be 5 % (Gamarra Lezcano et al. 2018). *Tn (%)* and *Tn* are total nitrogen in percentage (%) and gram Tn per kg of soil. *Sw* is soil weight in kg and was calculated from the measured bulk density and volume of the soil horizon used (m^2*0.3m).

Soil organic carbon (SOC) represents the organic carbon fraction in the soil, bound to soil organic matter (SOM). SOC was calculated using Equation 7.

$$SOC = SOM * 0.58 \quad (7)$$

The organic carbon content of the soil was assumed to be 58% (Rakshit et al. 2021). SOC represents grams of soil organic carbon per kilogram of soil, while SOM represents grams of soil organic matter per kilogram of soil.

The carbon-to-nitrogen ratio (C/N ratio) describes the ratio of carbon to nitrogen in soil organic matter, which was calculated using Equation 8. *Tn* is the total nitrogen Tn per kg of soil and SOC is the total soil organic carbon (g) per kg of soil.

$$(C/N)\text{ratio} = SOC/Tn \quad (8)$$

Table 2. Soil chemical and physical characteristics (0-30 cm).

physical		organic (g kg^{-1})		chemical (mg kg^{-1})		chemical (cmol kg^{-1})	
bulk density	1.4	C Oxid	17.4	P	64.4	Ca	18.3
sand (%)	5.9	SOM	39.5	Fe	1.6	Mg	6.2
silt (%)	36	Tn	1.8	Mn	54.5	K	0.7
clay (%)	57	SOC	22.9	Cu	0.3	Na	0.2
soil type	clay			Zn	2.5	Al	NA
pH	8.1			B	1		
C/N ratio	13			S	20.1		

C Oxid: oxidizable carbon, SOM: soil organic material, Tn: Total nitrogen, represents the nitrogen fraction in the soil, C/N ratio: represents the ratio of carbon to nitrogen in the soil organic material

2.3.2 Rice grain yield

The rice grain harvest (27.8 % mean-water content) with the husk still attached was performed on the 12th of May from both rice cultivars (Fig. 1b) after the field had been drained for 25 days for soil drying. The whole plot was mechanically harvested using a Kubota DC 105 X combine harvester, and each of the plots was harvested separately to determine the total weight and harvest moisture of the rice grains.

2.3.3 Koronivia grass root and above-ground biomass

The above-ground biomass of koronivia grass was harvested on 02nd June from both koronivia grass cultivars (Fig. 1b), by manually cutting the grass at ground level. Four frames of 50 x 50 cm were placed in the plot, and all the biomass within the frames was collected (Fig. 6a). Samples were oven-dried, and stem, and leaf were hand separated and weighted to determine the leaf/stem ratio (Smart et al. 2001). Grass root biomass weight was assessed by collecting soil cores (3.8 cm diameter

x 40 cm length) on 02nd June 2023 (Fig. 6c). The sampling procedure consisted of placing a frame (50 x 50 cm) on the soil four times per plot. Then, five samples were collected from each frame, as shown in Fig. 6 (a, b).

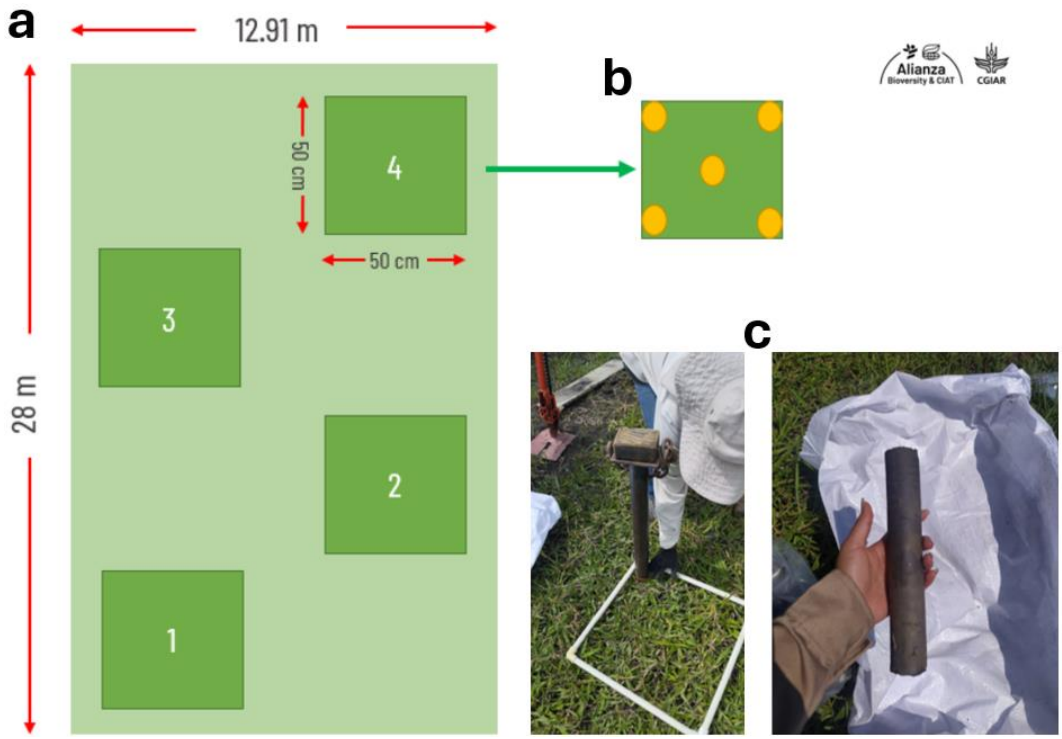

Fig. 6. Koronivia grass biomass sampling method. (a) placement of frames (50 x 50 cm) within each plot, in which above and below-ground biomass was collected. (b) Placement within each frame where the core samples were collected. (c) Demonstration of soil sample procedure and soil core, (Mildred Mayorga. 2024)

2.3.4 GHG sampling and measurements

The methods used to collect the gas emissions consisted of Static chamber method described in Alves et al. (2012). The white-painted polyvinyl chloride (PVC) chambers consisted of a base permanently inserted into the soil and a chamber top placed during gas collection. A small chamber was used for the koronivia grass, and a larger chamber was used for the rice experiment (with specifications in Table 3, Fig. 7). The chambers used for gas collection from the koronivia grass experiment used a rubber skirt to create a seal between the two parts (Fig. 7b). The chambers used for the rice experiment were bigger, and a water lock was used to create a seal between the two parts; in addition, the top contained a small fan to homogenize the air inside the chamber during sample collection.

Table 3. Koronovia grass and rice GHG-chamber specifications, dimensions, volume (base + chamber), and height. The insertion depths do not contribute to the chamber volume.

Characteristics	Chamber rice	Chamber forage
Chamber type	base + chamber	base + chamber
Chamber height (cm)	81	26
Base height (cm)	22	10
Insertion depth of base (cm)	10	2.5
Area (cm^2)	1194	495
Volume (base + chamber, dm^3)	123	18

Gas-sample collection interval for both the rice and forage grass experiment varied depending on fertilization management (see arrows in Fig. 3 and Fig. 4).

The rice experiment's GHG emissions collection started on 8th February and continued until 4th May, with a total of 16 weeks and 19 GHG-sample sessions. Samples were taken at a two-week interval unless fertilized. When fertilized, one the day before fertilizer application and continued for three consecutive days, resulting in four days in total, followed by one sampling per week for three weeks, as shown in Fig. 3.

The koronivia-grass experiment's GHG emissions collection started on 8th March and continued until 7th June, with a total of 13 weeks and 8 GHG-sample sessions, the distribution of GHG-sample sessions over the sampling period was dictated by the fertilization events since emissions were expected to increase after fertilizer application (Smith & Dobbie 2002). The experiment was fertilized once at the start of the collection period and sampling started the day after fertilizer application and continued for three consecutive days, followed by one sampling per week for three weeks. The two remaining sampling sessions had an increased interval of two and eight weeks, as shown in Fig. 4.

Fig. 7. Picture of greenhouse gas collection chambers. (a) Picture of greenhouse gas collection chamber used in the rice experiment, including chamber and base, over-pressurizing valve, thermometer, and air homogenizer (fan) battery. (b) Picture of greenhouse gas collection chamber used in the koronivia grass experiment, including chamber and base, rubber seal, and thermometer

Chambers tops were installed between 07:00 and 11:00 am to use the daily mean temperature during sampling, making it possible to quantify the total daily emission from the collected GHG samples (Alves et al. 2012). Directly after the chamber top was placed on the base, one gas sample was collected, and additional samples were collected 15, 30, and 45 minutes after installing the chambers, resulting in four samples that captured the gas emissions from the soil. Gas sample collection from the chambers was done by taking 15ml of gas through a septum, using a polypropylene syringe, and stored in 5.9ml vacuum vials, creating a positive pressure as shown in Fig. 7 and described by Arias-Navarro et al. (2013).

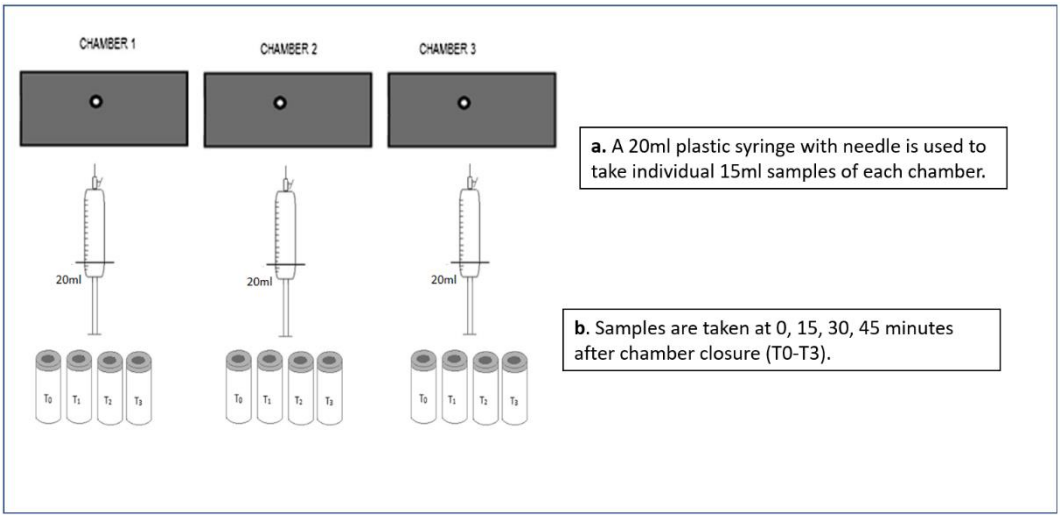

Fig. 7. Concept describing gas sample process from the GHG chambers, used in rice and koronivia grass experiment. Source: adapted from (Arias-Navarro et al. 2013)

Quantification of GHG in samples was done using gas chromatography (GC-2014 SHIMADZU gas chromatograph) equipped with a flame ionization detector (FID), electron capture detector (ECD), and methanizer. Certified standards were used for gas concentration analysis (Scotty® Analyzed Gases for CO_2: 2000 ppm, CH_4: 10 ppm and N_2O: 1 ppm, Analytical Accuracy +/- 5%).

Flux calculations were performed for both CH_4 and N_2O emissions by converting the GHG- emissions from ppm to g m^{-2} h^{-1} by using equation (1), (Costa et al. 2022).

$$Flux = \frac{dN2O}{dt} X \frac{V.M}{A.Vm} \quad (1)$$

Where *Flux* is gas emission rate (mg N_2O-N m^{-2} h^{-1}, or mg CH_4 m^{-2} h^{-1}), dN_2O/dt is the gas accumulation rate inside the chamber (ppm h^{-1}), *A* is the chamber base-area (in meters), *V* is the chamber volume (cubic meter), *M* is the gas molar mass (g mol^{-1}), V_m is molecular volume (dm^3 mol^{-1} at 10ºC) (Costa et al. 2022).

The fluxes were converted to daily emissions, assuming a constant emission rate over 24h. Linear interpolation of daily emissions was used to calculate cumulative CH_4 and N_2O emissions between two time points, using equation (2).

$$Cumulative\ Dflux = \frac{(Dflux\ 1 + Dflux2)}{2} X (t2 - t1) \quad (2)$$

Where D*flux* is the daily emissions, *Cumulative Dflux* is the cumulative GHG emission, and *t* is the time points of daily emission. The cumulated emission values from each time interval (*Cumulative Dflux*) were summed up to calculate the total

cumulative emission covering the whole sampling period (Costa et al. 2022) of 85 days in the rice experiment and 91 days in the koronivia grass experiment.

The index global warming potential (GWP) was used. GWP is used to define the cumulative radiative forcing from a unit of gas molecule over a time period, often 100 years, to reflect the pre-industrial conditions (Solomon et al. 2007). CO_2 is generally used as a reference gas in GWP estimation, and CH_4 and N_2O emissions are converted to CO_2 equivalents using their GWP. Based on a 100-year period, the GWP for CH_4 is 25, and for N_2O is 298 when the GWP of CO_2 is 1 (Camargo et al. 2018).

To estimate the combined global warming effect from the cumulative CH_4 and N_2O emissions in the rice and koronovia grass experiments, partial global warming potential (pGWP) was used. pGWP represents the combined radiative forcing potential of methane and nitrous oxide emitted from the soil. The pGWP was calculated by multiplying cumulative CH_4 and N_2O emission (CH_4 + N_2O *Cumulative Dflux*) from the experiments by their respective emission factor, using equation (3) (Camargo et al. 2018).

$$pGWP = (CH4 \times 25) + (N2O \times 298) \quad (3)$$

Where *pGWP* is the partial global warming potential (kg CO_2 eq ha^{-1}), the cumulative emissions (kg ha^{-1}) of methane (CH_4) and nitrous oxide (N_2O) (Camargo et al. 2018).

Yield-scaled pGWP (YpGWP) was used to understand the amount of emitted pGWP per kg of harvest where YpGWP (kg CO_2 eq kg^{-1} yield) is the ratio between pGWP and harvest yield, calculated using equation (4).

$$YpGWP = \frac{pGWP}{Y} \quad (4)$$

Where *YpGWP (yield-scaled global warming potential)* is the partial global warming potential (kg CO_2 eq ha^{-1}), and *Y* is the harvest yield (kg ha^{-1}) (Camargo et al. 2018).

2.4 Statistical analysis

The differences in average daily emissions and variation size between the cultivars were assessed in both the rice and koronivia grass experiments, which were performed to understand the methane and nitrous oxide emission flux patterns from the soil. For rice, the emission flux collection period was divided into three intervals: interval one (days 42-55), two (days 62-76), and three (days 83-127), as displayed in Fig. 3. In the forage grass experiment, the emission flux collection period was divided into two intervals interval, interval one (days 54-61) and interval two (days 69-145), and displayed in Fig. 4.

The statistical analysis for emission flux data within each interval (interval data) is shown in Fig. 8, was carried out to test for normality and homogeneity of variance. Shapiro-wilks normality test was used to test for normality, which evaluates if groups of data came from a common normal distributed population, and Levene´s homogeneity of variance test was used to assess if the different groups of data had equal variance (Owino et al. 2020).

Rice experiment emission comparisons within the sample periods (Fig. 3) were compared using the variance size for methane and nitrous oxide emissions and were performed as described in Fig. 8. The variance size comparisons had normal distribution and equal variance and were analyzed for significant differences using a t-test.

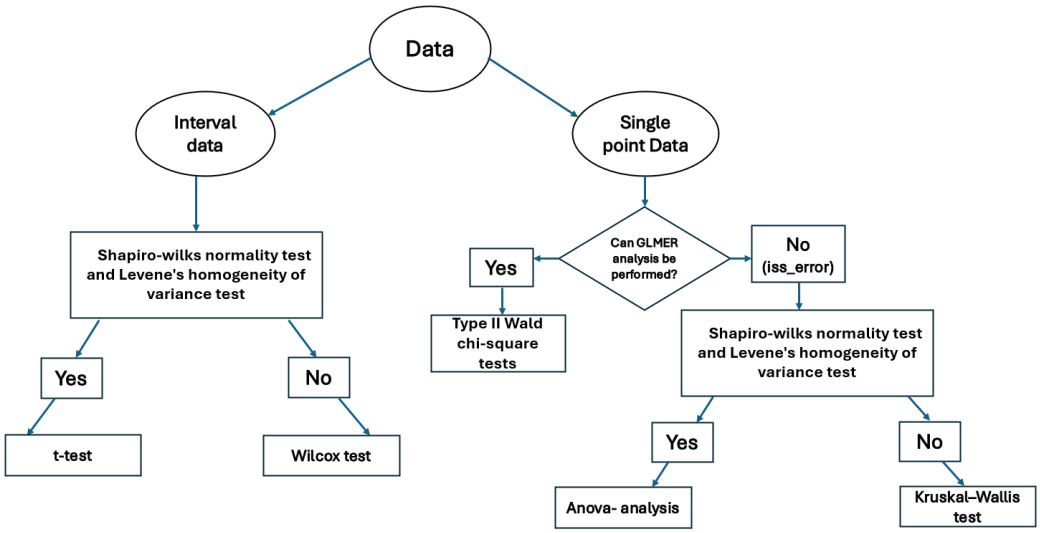

Fig. 8. Decision steps in the statistical analysis. Interval data statistical steps for mean and variance size for emission flux data, compared within the intervals. Single point data statistical steps for potential differences in rice grain yield and koronivia grass biomass production parameters (total biomass, biomass of leaf, root, stem, ratio of above and below ground biomass). The greenhouse gas parameters, cumulative methane and nitrous oxide emission for rice and koronivia grass, methane and nitrous oxide emission fluxes between the cultivars in rice and koronivia grass experiment, pGWP and YpGWP for both rice and koronivia grass

For single point analyzed data, a few statistical steps were performed, as shown in Fig. 8. A generalized linear mixed-effects model (GLMER) from the LME4 R-package was used and allows for the modeling of complex relationships in data when the data is not normally distributed or with equal variance and has different levels of grouping (Stoffel et al. 2017). Type II Wald chi-square tests were then used to investigate significant differences in the results of the GLMER- analysis, with the null hypothesis (H0) $p > 0.05$ and the alternative Hypothesis (H1) $p \leq 0.05$.

GLMER and type II Wald chi-square tests were used to evaluate and understand the potential differences in koronivia grass biomass production parameters, including biomass of leaf, total biomass, and the ratio of above and below-ground biomass. The greenhouse gas parameters including cumulative methane emission for both rice and koronivia grass and cumulative nitrous oxide emission (koronivia grass), methane and nitrous oxide emission fluxes between the cultivars in both rice and koronivia grass experiment, pGWP and YpGWP for both rice and koronivia grass.

When the use of GLMER- analysis was not possible due to singular fit error, meaning that one or more random effects in the model show no variability, causing estimates of zero variance in the random effects, this can cause adverse consequences for interference (Bates et al. 2018). Singular fit error happened for the following parameters: rice grain yield, rice cumulative nitrous oxide emission, and koronivia grass biomass production parameters, including root and stem biomass, for which Shapiro-wilks normality test and Levene´s homogeneity of variance test was used (Owino et al. 2020). The variance was equal and normally distributed for rice cumulative nitrous oxide emission, which allowed for the statistical test ANOVA- analysis of means. However, ANOVA has as requirements that the variance of values (homogeneity of variance) between different groups being compared needs to be similar and that the distribution of values within the groups needs to be normally distributed (Vik 2013). Rice grain yield and koronivia grass biomass production parameters, including root and stem biomass, did not fulfill the requirements for ANOVA, and non-parametric Kruskal–Wallis test was used, which can handle data with unequal variance (Ruxton 2006), with the null hypothesis (H0) $p > 0.05$, Alternative Hypothesis (H1) $p \leq 0.05$.

3. Results

Normal distribution and equal variance were not fulfilled for mean value comparisons within intervals and between each day of the sampling period for methane and nitrous oxide in the rice experiment. Likewise, normal distribution and equal variance were not fulfilled for koronivia grass (mean value comparisons within intervals between each day of the sampling period and Interval comparisons of variance size for both methane and nitrous oxide), forcing the use of Wilcoxon rank-sum test (Sainani 2012). Both the t-test and the Wilcoxon test had the null hypothesis (H0) $p > 0.05$ and alternative Hypothesis (H1) $p \leq 0.05$ (Sainani 2012).

3.1 Rice

3.1.1 Rice grain yield

Gran yield from rice cultivars HL23 and FE60, when harvested from the experimental plots, contained 27.5% mean water content; the total grain weight with 15% mean water content was calculated for comparisons with other studies. The grain yield differed significantly (p-value 0. 00029) between the cultivars, with HL23 producing 6.25 ton ha^{-1} of grains, while FE60 yielded 5.33 ton ha^{-1} (15 % mean water content, husk included) (Fig. 9).

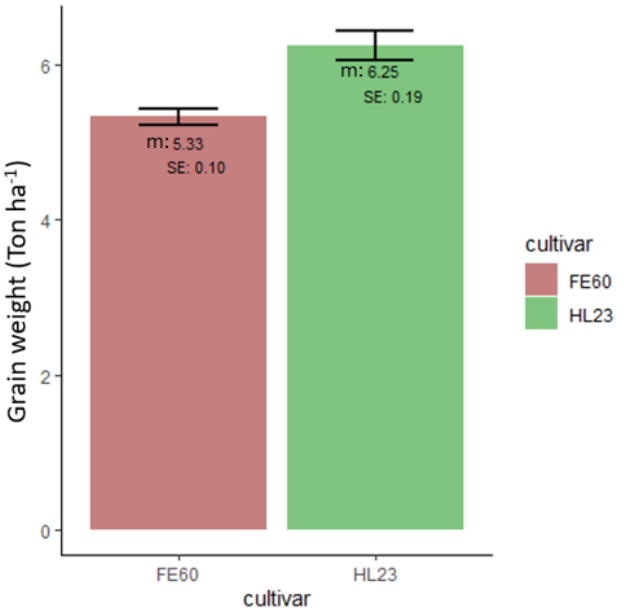

Fig. 9. Rice grain yield harvest (ton ha^{-1}), with 15% mean water content and husk included in cultivars HL23 and FE60. The displayed values (ton ha^{-1}) are means (m) (n=9) and the bar indicates the standard errors (SE)

3.1.2 Cumulative rice CH_4 emissions, fluxes, and interval comparisons

Cumulative methane emission (Fig. 10a) was evaluated by calculating CH_4 (kg ha^{-1}) from GHG samples, covering the whole sample period (between days 42-127 after sowing). The cumulative methane emission amount did not differ significantly between the rice cultivars HL23 (10.42 kg ha^{-1}) and FE60 (10.62 kg ha^{-1}).

Emission fluxes of methane in Fig. 10 (b) display CH_4 emission values for HL23 (green) and FE60 (red) rice cultivars during the sampling period, which is divided into three intervals: interval one (days 42-55), two (days 62-76), three (days 83-127). Both cultivars follow the same emission profile, where the lowest emission values were observed on the first fertilization event (day 42) for both cultivars HL23 and FE60, with an emission rate of 1.5 and 1.3 mg m^{-2} d^{-1}, respectively. The fluxes increased continuously during the following fertilization events (days 48 and 62) until the first peak, observed at day 64. After the first emission peak, both cultivars flowered (day 68- 72), during which the emission values reduced slightly until the highest flux value, which was observed at the second emission peak, 83 days after sowing for both cultivars HL23 and FE60, with an emission rate of 22.0 and 26.7 mg m^{-2} d^{-1}, respectively. After the second peak (day 83), the fluxes drop to values close to the initial emission levels for HL23 and FE60 by 76 % and 71 %, respectively, compared to the second peak. The third and final emission peak was detected on day 114 for both cultivars HL23 and FE60, with an emission rate of

11.7 and 10.7 mg m^{-2} d^{-1}, respectively. It was also observed that the fluxes for both cultivars at this period were lower than in the first two detected peaks.

The average daily emissions of each cultivar in each of the three sampling intervals (42-55, 62-76, and 83-127 days after sowing) are shown in Fig. 10 (c). In interval one, cultivar FE60 had a significantly lower methane emission mean value than HL23. To investigate further which days caused the significant difference, a mean value comparison for each day was done (appendix Fig. 19), evidencing that cultivar FE60 had significantly lower emission values only on days 43 and 45; no significant difference was found for any day in intervals two and three.

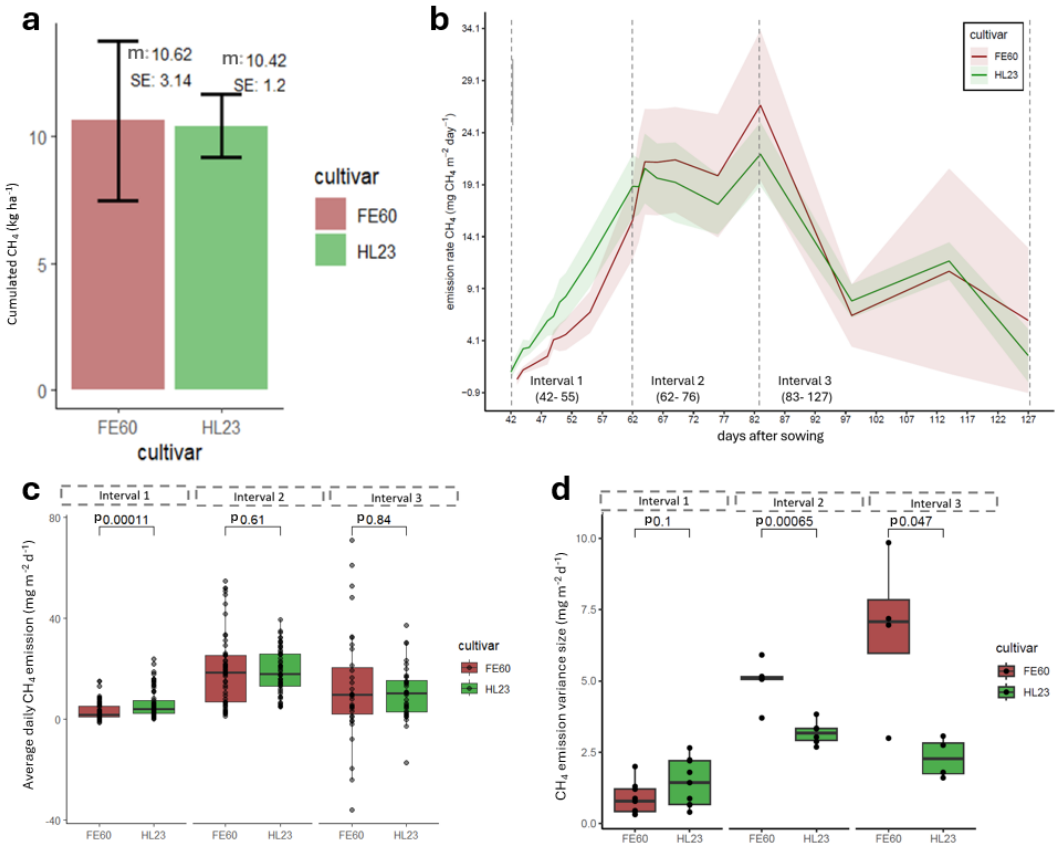

Fig. 10. Dynamics of methane emissions according to different rice cultivars and in different sampling intervals. (a) Cumulative emission of methane with mean value (m) (n=9) and the bar indicates the standard error (SE) for the complete sampling period (days 42 - 127). (b) Emission fluxes of methane were observed at three intervals (days after sowing). Green and red lines represent the average flux of each rice cultivar. The light-colored area represents the standard error (SE) from the flux average (n=9). (c) In the Boxplot of Methane emission flux, 50 % of data is found in the colored box, the line represents the median, n equal 9, 6 and 4 for Interval I, II and III, respectively, and the dots not connected by the whiskers are outliers. Comparisons were performed within the three intervals; each interval shows the average daily methane emission for both cultivars. The Wilcoxon test was conducted between both cultivars in each interval and the significance is shown as a p-value. (d) Individual dots show the standard error (SE) for the average daily methane emission in each interval. Boxplot shows the mean distribution of all the standard errors in the interval and n equal 9, 6 and 4 for Interval I, II and III, respectively. A t-test was performed between both cultivars in each interval, and the significance is shown as a p-value

The same intervals were used to see if there was a difference in the variance size between the cultivars to understand better the consistency in the cultivar emission pattern, with a comparison of methane emission flux standard error being performed within each interval (Fig. 10d). The standard error for cultivars HL23 and FE60 was grouped in the three intervals, which showed that cultivar FE60 had a significantly higher variance in intervals two and three.

3.1.3 Cumulative rice N_2O emissions, fluxes, and interval comparisons

Cumulative nitrous oxide emission (Fig. 11a) was evaluated by calculating N_2O (kg ha^{-1}) from GHG samples, covering the whole sample period (between days 42-127 after sowing). The cumulative nitrous oxide emission amount did not differ significantly between the rice cultivars HL23 (0.08 kg ha^{-1}) and FE60 (0.16 kg ha^{-1}).

Emission fluxes of nitrous oxide in the Fig. 11 (b) display N_2O emission values for HL23 (green) and FE60 (red) rice cultivars during the sampling period, which is divided into three intervals: intervals one (days 42-55), two (days 62-76), three (days 83-127).

Both cultivars partially followed the same emission profile, with emission peaks corresponding to some of the fertilization events. The first emission peak for both cultivars was at the first fertilization event on day 43 after sowing. The second emission peak (day 51) was four days after the second fertilization event (day 48), and the third peak for cultivar HL23 (Day 62) corresponds to the third fertilization event. Both cultivars had an additional fourth peak, where the highest flux value was observed at day 66 for FE60 (1.21 mg m^{-2} d^{-1}) and day 69 for HL23 (1.24 mg m^{-2} d^{-1}), which was around the date of flowering (6-10 March).

The lowest flux value was observed for cultivar HL23 (-0.68 mg m^{-2} d^{-1}) at day 83 and remained below emission value 0 for the rest of the sample period (day 127). The lowest flux value was observed for cultivar FE60 (-0.21 mg m^{-2} d^{-1}) on day 98.

The average daily emissions of each cultivar in each of the three sampling intervals (42-55, 62-76, and 83-127 days after sowing) are shown in Fig. 11 (c), showing no significant difference between the cultivars within the intervals. To investigate further if any day showed a significant difference, a mean value comparison for each day was done (appendix Fig. 20), evidencing that cultivar FE60 had a significantly lower value on day 43; no significant difference was found for any day in intervals two and three. The same intervals were used to see if there was a difference in the variance size between the cultivars to understand better the consistency in the cultivar emission pattern, with a comparison of nitrous oxide emission flux standard error being performed within each interval (Fig. 11d). The

standard error for cultivars HL23 and FE60 was grouped in the three intervals, which were compared, showing no significant difference in variance.

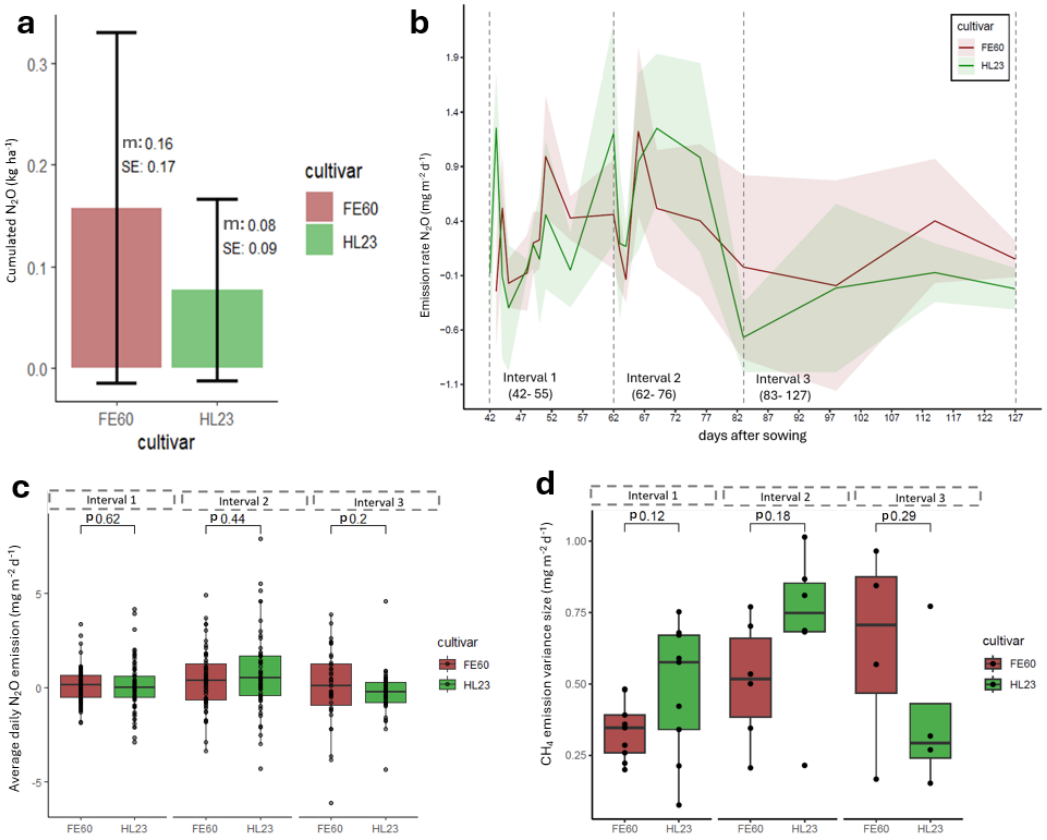

Fig. 11. Dynamics of nitrous oxide emissions according different rice cultivars and sampling intervals. (a) Cumulative emission of nitrous oxide with mean value (m) (n=9) and the bar indicates the standard error (SE) for the complete sampling period (days 42 - 127). (b) Emission fluxes of nitrous oxide were observed at three intervals (in days after sowing). Green and red lines represent the average flux of each rice cultivar. The light-colored area represents the standard error (SE) from the flux average (n=9). (c) In the boxplot of nitrous oxide emission flux, 50 % of data is found in the colored box, the lines represent the median, n equal 9, 6 and 4 for Interval I, II and III, respectively and the dots not connected by the whiskers are outliers. Comparisons were performed within the three intervals; each interval shows the average nitrous oxide emission for both cultivars. The Wilcoxon test was conducted between both cultivars in each interval, and the significance is shown as a p-value (p). (d) Individual dots show the standard error for the average daily nitrous oxide emission in each interval. Boxplot shows the mean distribution of all the daily standard errors in the interval, n equal 9, 6 and 4 for Interval I, II and III, respectively. A t-test was performed between both cultivars in each interval, and the significance is shown as a p-value (p)

3.1.4 Rice cultivation partial global warming potential (pGWP) and yield -scaled partial global warming potential (YpGWP)

Partial global warming potential (pGWP) was calculated by combining the radiative forcing potential of methane and nitrous oxide emitted from the soil (Fig. 12a). Mean values for cultivars HL23 and FE60, 283.4 kg CO_2 eq ha^{-1} and 312.7kg CO_2

eq ha^{-1}, respectively, did not differ significantly between the cultivars. Yield-scaled partial global warming potential (YpGWP) was calculated by combining the radiative forcing potential of methane and nitrous oxide emitted from the soil, divided by the rice grain yield (kg ha^{-1}) with 15% moisture content (Fig. 12b). Mean values for cultivars HL23 and FE60, 0.04 kg CO_2 eq. kg^{-1}rice and 0.06 kg CO2 eq. kg^{-1}rice, respectively, did not differ significantly between the cultivars.

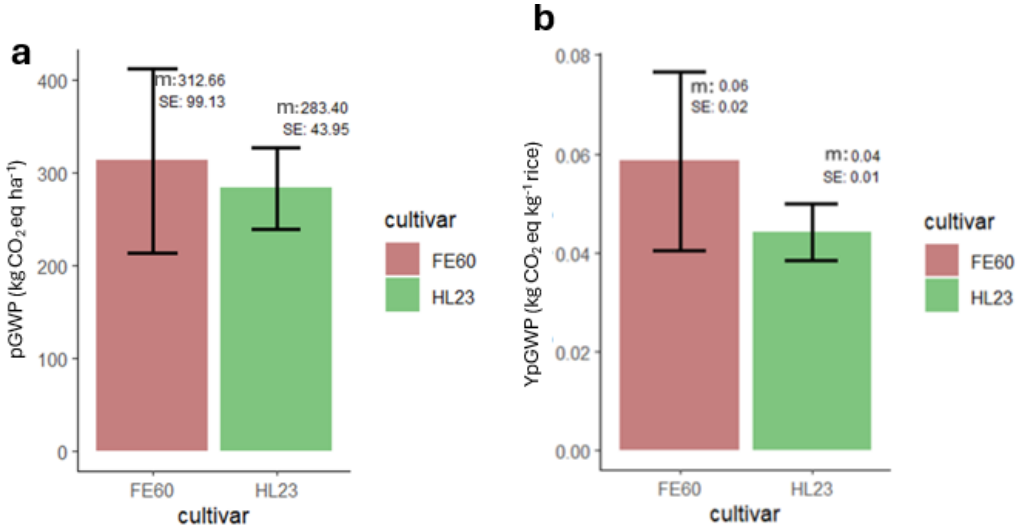

Fig. 12. Cumulative radiative forcing from GHG emissions derived from rice experiment. (a) Partial global warming potential (pGWP) (kg CO_2 eq ha^{-1}), calculated from cumulative CH_4 and N_2O emissions. (b) Yield – scaled pGWP (YpGWP) (kg CO_2 eq kg^{-1} rice), calculated from the cumulative CH_4 and N_2O emissions per kg rice grain yield (15% water content). values are means (m) (n=9) and the bar indicates the standard error (SE)

3.1.5 Rice GHG emission principal component analysis (PCA)

A Principal Component Analysis (PCA) was performed to understand better the effect of the different environmental variables that can contribute to the CH_4 and N_2O emissions profile. Vectors further away from the center indicate a bigger contribution to the overall variance, and vectors clustered together have a stronger positive effect on the values of other vectors in the cluster.

The PCA addressing methane emission rates (CH_4_ER) shows that the first component explains 55 % of the variance (Fig. 13a). Methane emission rates were grouped with total nitrogen, oxidizable carbon, and soil organic carbon, all related to organic matter, and negatively correlated with the plot and the soil factors percentage of sand and silt. In the second component, explaining 13 % of the variance, the methane emission rate was grouped with water content and negatively correlated with percentual clay content. However, no connections were perceived as strong enough to influence emissions or further investigation.

The PCA addressing nitrous oxide emission rates (N_2O_ER) shows that the first component explains 51 % of the variance; sand, silt plot, and pH were negatively

correlated with soil organic carbon, total nitrogen, oxidizable carbon, and clay content (Fig. 13b). On the second component, explaining 14 % of the variance, water content, and saturation extract was negatively correlated with pH. The nitrous oxide emission rate was grouped with chamber and soil temperature, all located close to the center of the PCA. The position of nitrous oxide emission rates indicates a low contribution to the total variation observed in the data.

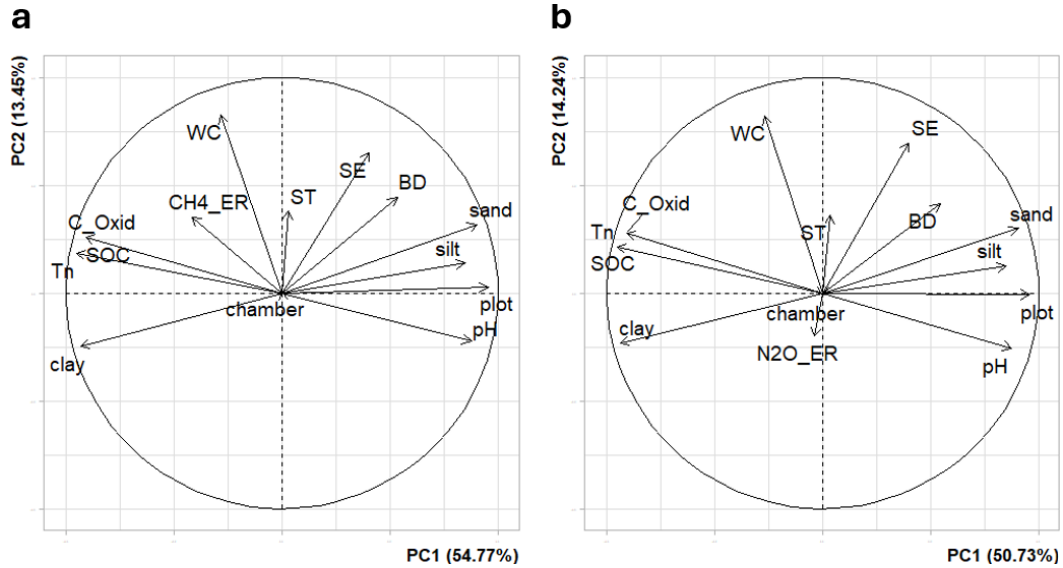

Fig. 13. Principal component analysis (PCA) loadings plots for (a) methane (CH4_ER) and (b) nitrous oxide emission rates (N2O_ER). With the vectors emission collection chamber (chamber) and experiment plots (plots). Soil parameters bulk density (BD), water content (WC), saturation extract (SE), soil temperature (ST), pH, soil available carbon (SOC), oxidizable carbon (C-Oxid), total nitrogen (Tn), percentage of silt, sand, and clay

3.2 Koronivia grass

3.2.1 Koronivia grass above and below ground biomass production

Above-ground biomass and root biomass production for both koronovia grass cultivars BH08 and CI67 (Fig. 14 a-e) was evaluated by comparing the dry weight (g m^{-2}) of leaf, stem, root, and the combined dry weight (leaf, stem, and roots (g m^{-2})). No difference between the biomass of cultivar BH 08 and CI67 (above-ground, root biomass or root – above-ground biomass) and the dry weight ratio between root and above-ground biomass ratio was observed. The results indicate that no dry weight comparison differed significantly between the cultivars.

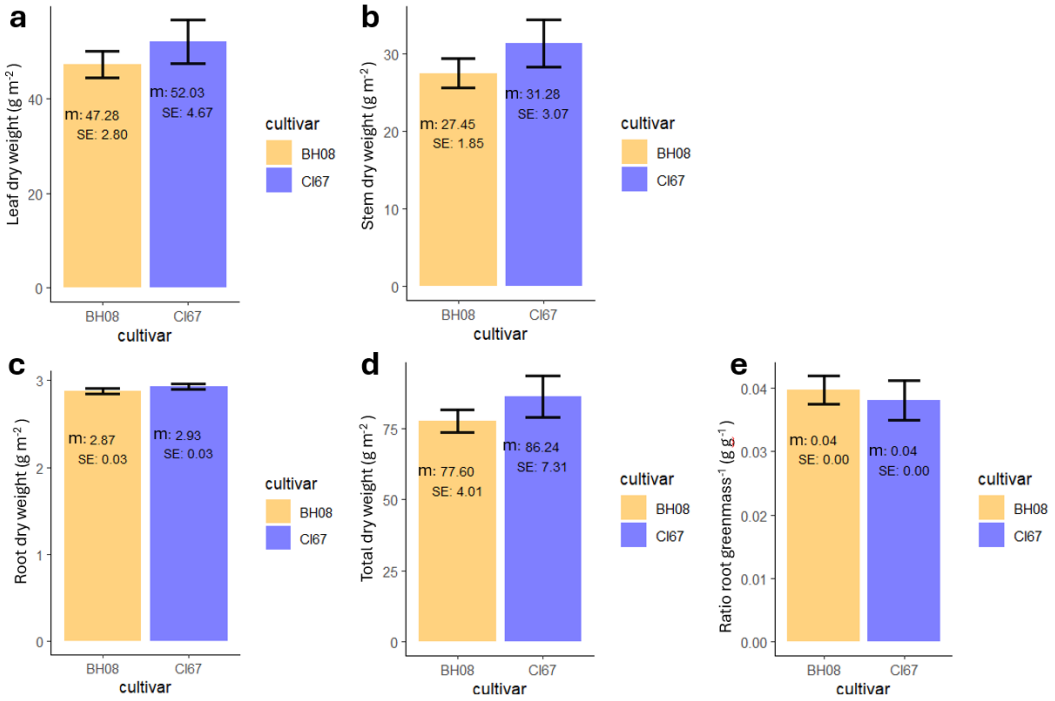

Fig. 14. Comparison of biomass production in dry weight, between the two koronivia grass cultivars BH08 and CI67. (a) Leaf dry weight (g m^{-2}), (b) stem dry weight (g m^{-2}), (c) root dry weight (g m^{-2}), (d) total dry weight (g m^{-2}), (e) ratio dry weight root/above-ground biomass (dry weight) (g g^{-1}). Values are means (m) (n=9) and the bar indicates the standard error (SE)

3.2.2 Koronivia grass cumulative CH_4 emissions, fluxes, and interval comparisons

Cumulative methane emission (Fig. 15a) was evaluated by calculating kg CH_4 (kg ha^{-1}) from GHG samples covering the whole sample period (between days 54 - 145 after field-planting). The cumulative methane emission amount did not differ significantly between the koronivia grass cultivars BH08 (0.11 kg CH_4 ha^{-1}) and CI67 (0.28 kg ha^{-1}).

Emission fluxes of methane displayed CH_4 emission values for BH08 (orange) and CI67 (blue) koronivia grass cultivars during the sampling period, divided into two intervals: interval one (days 54-61) and interval two (days 69-145), (Fig. 15b). Both cultivars partially followed the same emission profile, where the lowest methane emission value was observed for cultivar BH08 at the beginning of the sample period at day 55 (-0.18 mg CH_4 m^{-2} d^{-1}). Cultivar CI67 (-0.07 mg m^{-2} d^{-1}) displayed the lowest value on the last sample day (145). The highest value was observed for cultivar CI67 (1.52 mg m^{-2} d^{-1}) at the emission peak 61 days after planting in the field and seven days after fertilizing. After the emission peak, the emission rate for CI67 decreased continuously during the rest of the sample period. The highest observed emission value for cultivar BH08 (0.33 mg m^{-2} d^{-1}) was 61 days after planting in the field and remained elevated in a plateau for eight days

(until day 69). The emission rate for BH08 decreased from day 69 to 75; after day 75, the emission rate increased until the end of the sample period.

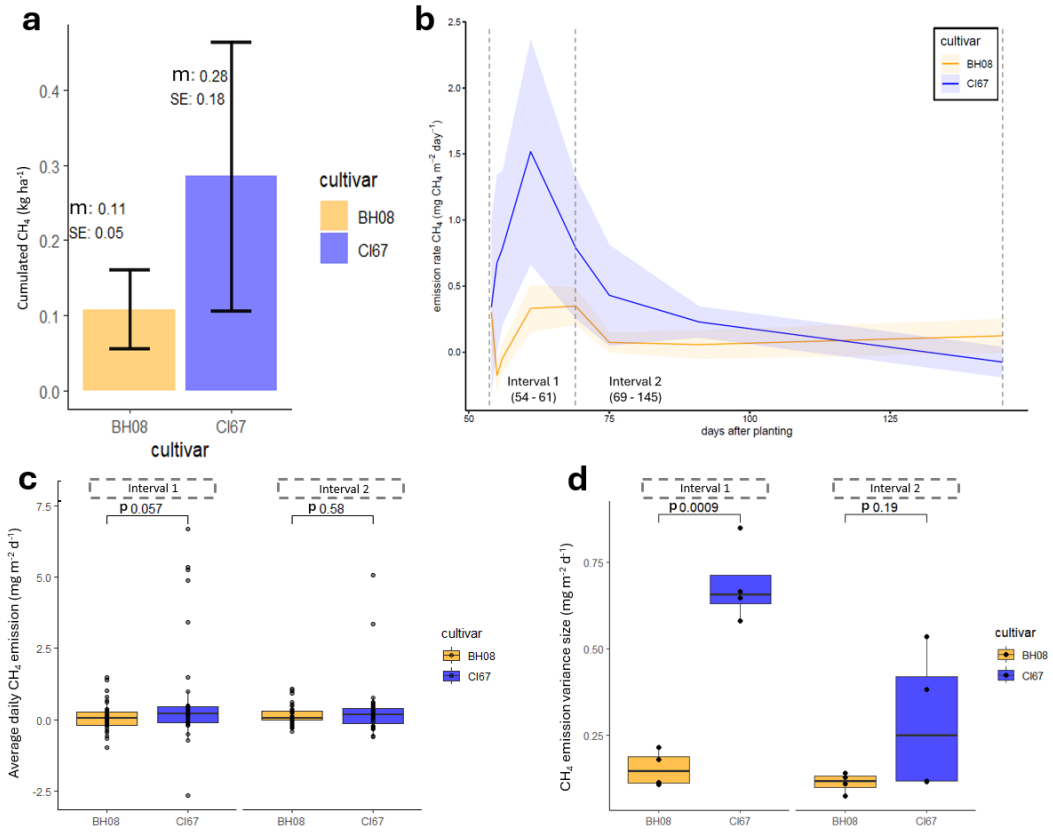

Fig. 15. Dynamics of methane emissions according different koronivia grass cultivars and in different sampling intervals. (a) Cumulative emission of methane with mean value (m)(n=9) and the bar indicates the standard error (SE) for the complete sampling period (days 54 - 145). (b) Emission fluxes of methane observed at two intervals (in days after planting in the field). Lines represent the average flux of each koronivia grass cultivar. The light-colored area represents the standard error (SE) from the flux average (n=9). (c) Boxplot of methane emission flux, 50 % of data is found in the colored box, the line represents median, n equal 9, 6 and 4 for Interval I, II and III, respectively and the dots not connected by the whiskers are outliers. Comparisons were performed within the two intervals; each interval shows the average daily methane emission for both cultivars. The Wilcoxon test was conducted between both cultivars in each interval and the significance is shown as a p-value (p). (d) Individual dots show the standard error for the average daily methane emission in each interval. Boxplot shows the mean distribution of all the standard errors in the interval and n equal 9, 6 and 4 for Interval I, II and III, respectively. The Wilcoxon test was performed on both cultivars at each interval, and the significance is shown as a p-value (p)

The average daily emissions of each cultivar in the two sampling intervals (days 54-61 and days 69-145) (Fig. 15c) showed no significant difference between the cultivars within the intervals. To investigate further which days caused the significant difference, a mean value comparison for each day was done (appendix Fig. 21). No significant difference was found for any day in both intervals one and two. The same intervals were used to see if there was a difference in the variance size between the cultivars to understand better the consistency in the cultivar

emission pattern, with a comparison of methane emission flux standard error being performed within each interval (Fig. 15d). The standard error for cultivars BH08 and CI67 was grouped in the two intervals, which were compared showing that cultivar CI67 had a significantly higher variance in interval one.

3.2.3 Koronivia grass cumulative N_2O emissions, fluxes, and interval comparisons

Cumulative nitrous oxide emission (Fig. 16a) was evaluated by calculating N_2O (kg ha^{-1}) from GHG samples, covering the whole sample period (between days 54-145 after field-planting). The cumulative nitrous oxide emission amount did not differ significantly between the koronivia grass cultivars BH08 (0.44 kg ha^{-1}) and CI67 (0.40 kg ha^{-1}).

Emission fluxes of nitrous oxide displayed N_2O emission values for BH08 (orange) and CI67 (blue) koronivia grass cultivars during the sampling period, divided into two intervals: interval one (days 54-61) and interval two (days 69-145), (Fig. 16b). The first N_2O emission peak for both cultivars BH08 and CI67 was observed two days after fertilizing and 55 days after planting in the field. The second and biggest emission peak for both cultivars, BH08 (2.55 mg m^{-2} d^{-1}) and CI67 (3.44 mg m^{-2} d^{-1}) was observed 61 days after planting in the field. The lowest observed value was at the end of the sample period, day (145) for both cultivars BH08 and CL67, with an emission rate of 0.09 and 0.03 mg m^{-2} $d^{-1,}$ respectively.

The average daily emissions of each cultivar in each of the two sampling intervals, one (54-61) and two (69-145 days after field planting) showed no significant difference between the cultivars within both intervals (Fig. 16c). To investigate further which days caused the significant difference, a mean value comparison for each day was made (appendix Fig. 22), no significant difference was found for any day in both intervals. The same intervals were used to see if there was a difference in the variance size between the cultivars to understand better the consistency in the cultivar emission pattern, with a comparison of nitrous oxide emission flux standard error being performed within each interval (Fig. 16d). The standard error for cultivars BH08 and CI67 was grouped in the two intervals, which showed no significant difference between the cultivars.

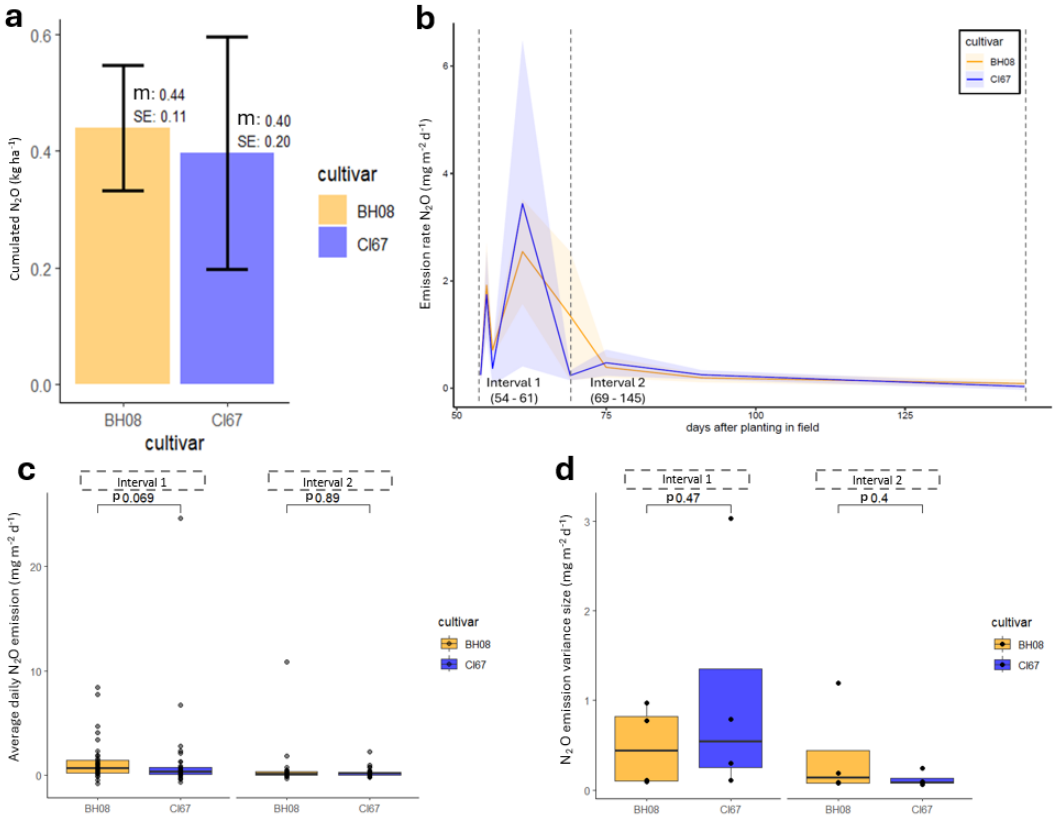

Fig. 16. Dynamics of nitrous oxide emissions according different koronivia grass cultivars and in different sampling intervals. (a) Cumulative emission of nitrous oxide with mean value (m) (n=9) and the bar indicates the standard error (SE) for the complete sampling period (days 54 - 145). (b) Emission fluxes of nitrous oxide were observed at two intervals (in days after planting in the field). Lines represent the average flux of each koronivia grass cultivar. The light-colored area represents the standard error (SE) from the flux average (n=9). (c) Boxplot of nitrous oxide emission flux, 50 % of data is found in the colored box, the line represents median, n equal 9, 6 and 4 for Interval I, II and III, respectively and the dots not connected by the whiskers are outliers. Comparisons were performed within the two intervals; each interval shows the average daily nitrous oxide emission for both cultivars. The Wilcoxon test was conducted between both cultivars in each interval and the significance is shown as a p-value (p). (d) Individual dots show the standard error for the average daily nitrous oxide emission in each interval. Boxplot shows the mean distribution of all the standard errors in the intervals and n equal 9, 6 and 4 for Interval I, II and III, respectively. The Wilcoxon test was performed between both cultivars in each interval and the significance is shown as a p-value (p)

3.2.4 partial global warming potential (pGWP) and yield -scaled partial global warming potential (YpGWP)

Partial global warming potential (pGWP) combines the radiative forcing potential of methane and nitrous oxide emitted from the soil (Fig. 17a). Mean values for cultivars BH08 and CI67, 133.9 kg CO_2 eq ha^{-1} and 125.3 kg CO_2 eq ha^{-1}, respectively, did not differ significantly between the cultivars. Yield-scaled partial global warming potential (YpGWP) combines the radiative forcing potential of

methane and nitrous oxide emitted from the soil, divided by the dried forage yield (stem + leaf), (kg ha^{-1}) (Fig. 17b). Mean values for cultivars BH08 and CI67, 0.17 kg CO_2 eq. kg^{-1} forage, and 0.14 kg CO_2 eq. kg^{-1} forage, respectively, did not differ significantly between the cultivars.

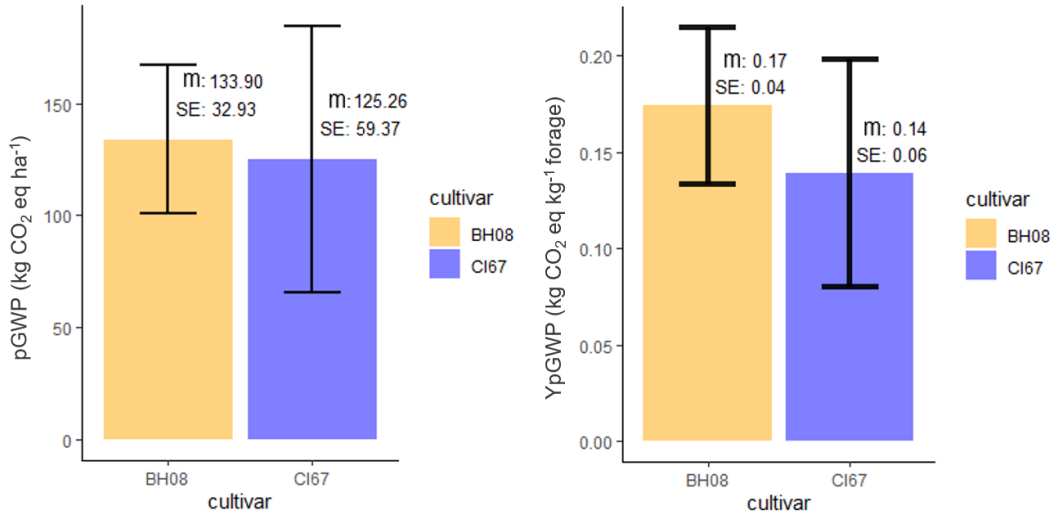

Fig. 17. Cumulative radiative forcing from GHG emissions derived from Koronovia grass experiment. (a) Partial global warming potential (pGWP) (kg CO_2 eq ha^{-1}), calculated from cumulative CH_4 and N_2O emissions. (b) Yield–scaled pGWP (YpGWP) (kg CO_2 eq kg^{-1} forage), calculated from the cumulative CH_4 and N_2O emissions per kg forage (above-ground dried biomass). Values are means (m) (n=9) and the bar indicates the standard error (SE)

3.2.5 Koronivia grass GHG emission principal component analysis (PCA)

A Principal Component Analysis (PCA) was performed to understand better the effect of the different environmental variables that can contribute to the CH_4 and N_2O emissions profile. Vectors further away from the center indicate a bigger contribution to the overall variance, and vectors clustered together have a stronger positive effect on the values of other vectors in the cluster.

The PCA addressing methane emission rates (CH_4_ER) showed that on the first component explains 46 % of the variance, where pH, sand, and bulk density were negatively correlated with soil organic carbon, total nitrogen, oxidizable carbon, and clay content (Fig. 18a). On the second component explaining 18 % of the variance, clay content was negatively correlated with soil organic carbon, total nitrogen, oxidizable carbon plot, and silt. The methane emission rates were grouped with chamber and precipitation, all located close to the center of the PCA. The position of methane emission rates indicates a low contribution to the total variance in the data. On the first component, pH, sand, and bulk density were negatively correlated with soil organic carbon, total nitrogen, oxidizable carbon, and clay content.

The PCA addressing nitrous oxide emission rates (N_2O_ER) showed that on the first component, which explains 45 % of the variance, soil organic carbon, total nitrogen, oxidizable carbon, and clay content were negatively correlated with pH, sand, bulk density, and plot (Fig. 18b). On the second component explaining 18 % of the variance, soil organic carbon, total nitrogen, oxidizable carbon, and clay content were negatively correlated with clay content. The nitrous oxide emission rates were grouped with chamber and precipitation close to the PCA's center. The position of nitrous oxide (N_2O_ER) indicates a low contribution of nitrous oxide emission rate to total variance in the data.

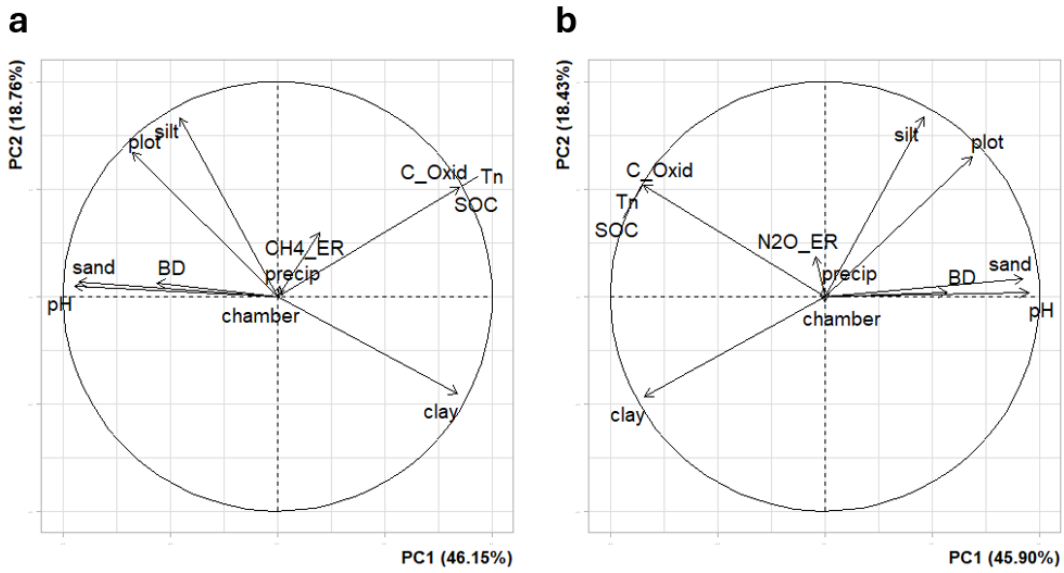

Fig. 18. Principal component analysis (PCA) loadings plots for (a) methane (CH4_ER) and (b) nitrous oxide emission rates (N2O_ER). With the vectors, emission collection chamber (chamber), experiment plots (plots), and precipitation (precip). Soil parameters include bulk density (BD), pH, soil available carbon (SOC), oxidizable carbon (C-Oxid), total nitrogen (Tn), and percentage of silt, sand, and clay

4. Discussion

4.1 Displayed differences in grain yield of rice cultivars

The rice grain yield is an important agronomic parameter since it is the primary product of rice cultivation for human consumption (Loaiza et al. 2024), and an important factor in YpGWP calculations. The rice grain yield showed a clear difference between the cultivars, with Cultivar HL23 having significantly higher grain production (Fig. 9). This higher comparative performance of HL23 was also observed by Perengüéz (2018) in a rice cultivar comparison. However, the significant difference is not present in the rice cultivar comparison of HL23 and FE60 by Baquero & Zambrano (2016), indicating that more production cycles and on-farm experiments are needed to corroborate these findings.

4.2 Effect of rice cultivar on N_2O and CH_4 emission profile

There was no significant difference between cultivars HL23 and FE60 when comparing cumulative CH_4 or N_2O emissions (Fig. 10a, Fig. 11a) indicating that the two cultivars have similar effects on total emissions, potentially due to comparable levels of root exudates (Baruah et al. 2010).

When comparing cumulative CH_4 emissions between the cultivars used in this experiment (Fig. 10a) to other experiments (such as Camargo et al. 2018; Oo et al. 2018), we see 10-60-fold lower emissions in this experiment; this big difference may be due to the sampling period, which covered 82 days in this experiment, while the referenced experiment GHG sampling was conducted over 106 (Oo et al. 2018) and 120 days (Camargo et al. 2018). Another contributing factor causing low emissions levels in our experiment may be the high clay content, which causes a relatively high entrapment of methane in the clayey soil. Potential cracks in the soil profile caused high water percolation speed, reducing methane emission (Malyan et al. 2016), the reduction of methane emission is caused by the higher redox potential, maintained by high percolation speed (Yagi et al. 1998), causing an unfavorable environment for the CH_4-producing bacteria (methanogens) (Malyan

et al. 2016). While the exact reasons for the relatively low CH_4 emission values are not clear, it has been observed in other similar experiments in Colombia, such as for Loaiza et al. (2024) showed similar values using a similar sampling method and experimental setup at a site in Tolima, relatively close to CIAT. They suggest that contributing factors may be due to drainage during the first 40-60 days after sowing (30 days in this experiment). The drainage stimulated methanotrophic archaea and bacteria activity, oxidizing CH_4 to CO2 (Malyan et al. 2016), and high redox potential (Pepper & Gentry 2015). According to Loaiza et al. (2024) increased oxygen availability in the soil increased sulfate and ferric iron concentrations, causing reduced survival rate and methanogenic activity of methane-producing archaea, even after the soil gets flooded and the redox potential drops. Loaiza et al. (2024) also mentioned a potential reduction of aerenchyma development in the young rice plants due to fewer anoxic conditions, aerenchyma are specialized cells that enhance the transportation of gas within the plant, and the potential reduction of aerenchyma causes decreasing CH_4 transportation through the plant tissue throughout the season. The reduction of aerenchyma can affect greatly since up to 90 % of methane emissions from the rice field are from rice aerenchyma-mediated transport (Wassmann & Aulakh, 2000).

When comparing cumulative N_2O emissions to other experiments, both cultivars appear to be in line with other experiments, ranging in values between -0.2 to 0.6 kg ha^{-1} (Camargo et al. 2018; Oo et al. 2018). The N_2O emission values also indicate that the factors potentially affecting CH_4 emissions did not affect the N_2O emissions.

When comparing the CH_4 emission rate between cultivars, we can see that the CH_4 emissions increased continuously during the three fertilization events included in the sampling period (Fig. 10b) until 20 days after the last fertilization event. The high methane emission is connected to fertilization events caused by the nitrate demand by type 2 methanogenic bacteria (Baruah et al. 2010). The emission rate was reduced six days after the last fertilization event (day 68-72), during which both cultivars flowered. After flowering, the emission increased, which may be caused by increased root exudate between flowering and maturation since Increased root exudate rate causes an increase in the growth of nitrifiers and denitrifiers (Baruah et al. 2010).

The comparisons of mean CH_4 emission between the cultivars within the intervals (Fig. 10c) show that cultivar FE60 had a significantly lower emission rate compared to HL23 in interval one, which covered the panicle differentiation stage, in which the rice plants switch from vegetative to reproductive development (Chen et al. 2019). The panicle differentiation stage causes high root growth and exudate rates (Li et al. 2022). The higher emission rate in cultivar HL23 could be an effect of higher root growth and exudate rate, which also creates a higher area for diffusion due to larger root biomass (Baruah et al. 2010) since 60-90 % of total CH_4 emission

from rice fields is through the rice plant (Kim et al. 2018). When comparing the cultivars in intervals two and three, no difference in emission rates was found, which could point to the potential difference of root growth in interval one, which had been reduced in the later stages of development.

When looking at the CH_4 emission variance (Fig. 10d), meaning how much the individual chambers within each cultivar differ from each other, there was no significant difference in interval one, showing a similar variation in growth pattern between both rice cultivars. In intervals two and three, the methane emission variance of cultivar FE60 was significantly higher than that of HL23. The highest difference between the cultivars was observed in interval two, which includes the CH_4-emission peaks and flowering of rice plants. The large difference in methane emission variance could indicate that cultivar FE60 displays higher variation in growth and development aspects that affect methane emission rate. Another reason could be that the slower-growing roots of FE60 encounter pockets of methane to a larger extent later in the growth period, causing a sudden local influx of methane emission (Baruah et al. 2010), while keeping the methane emission rate low in interval one.

The emission fluxes profile of N_2O (Fig. 11b) follows the same emission trend as methane emission fluxes (Fig. 10b) with most nitrous oxide emissions being released during fertilization and flowering. The four N_2O emission peaks align with the fertilization events and the flowering period (43, 49, 62 DAS), caused by the applied nitrogen fertilizer and increased root exudation, which agrees with other studies such as Baruah et al. (2010). The emission peaks show that nitrogen fertilization and flowering increase N_2O emissions due to increased bioavailable nitrogen and high root exudation of organic carbon (Baruah et al. 2010). The N_2O emissions did not drastically change after the irrigation stopped (DAS 110), potentially due to insufficient available nitrogen for the nitrification and denitrification-producing bacteria (Durango Morales et al. 2021a).

The comparisons of mean N_2O emission between the rice cultivars within the intervals (Fig. 11c) showed no significant difference within any of the intervals. Interval one, which included the panicle differentiation stage (Chen et al. 2019), showed that FE60 had a significantly lower mean N_2O emission on DAS 43 (appendix Fig. 20). The exact reason for the difference was hard to determine since it was at the beginning of the sample period, and we could not see how the emission pattern was earlier in the cropping season. However, the absolute value of the emissions was low, causing statistical significance with slight emission differences between cultivars, reducing the reliability of the statistical analysis.

When looking at the variance of N_2O (Fig. 11d), meaning how much the individual chambers within each cultivar differ from each other, no significant variance difference was found in any of the intervals. This lack of difference in variance of N_2O emissions between cultivars indicates that the rice cultivars had a

similar homogeneous growth pattern and development concerning nitrous oxide emission rate, while still displaying significant differences in relation to variance of CH_4 emission rate.

4.3 Combined climatic impact of CH_4 and N_2O emissions and grain yield

When comparing the pGWP and YpGWP from the grain yield and combined cumulated methane and nitrous oxide emissions (Fig. 12), a tendency for lower YpGWP can be observed for HL23 (Fig. 12 b) due to higher grain yield (Fig. 9). However, it was not large enough to be significantly different due to a lack of difference in cumulated emissions between the cultivars. However, yield can be essential to counterbalance the negative environmental impact.

When comparing these findings to the literature, the pGWP and YpGWP values (283-312 kg CO_2 eq ha^{-1}) presented in this report are compatible with the one found by Loaiza et al. (2024), but 10-50 fold lower than other sources (Table 4), (Bhattacharyya et al. 2013; Moterle et al. 2013; Bayer et al. 2014; Zschornack et al. 2016; Camargo et al. 2018; Oo et al. 2018). The reason largely depends on the short time of methane emission accumulation values presented in this work. Longer sampling seasons could have produce values that are less divergent from other sources.

Table 4. Partial global warming potential (pGWP) and yield-scaled global warming potential (YpGWP) values were observed in the field experiment and compared to other sources.

source	pGWP (kg CO_2 eq ha^{-1})	YpGWP (kg CO_2 eq kg^{-1} rice)
Experimental values	280-310	0.04 - 0.06
Loaiza et al., 2024	123-1361	-
Bhattacharyya et al., 2013	2500-3200	2.0-2.7
Camargo et al., 2018	4000-18000	0.5-2.4
Oo et al., 2018	2600-6000	0.6-1.0
Zschornack et al., 2016	2500-10500	0.2-0.9
Bayer et al., 2014	10300-13300	1.4-1.8
Moterle et al., 2013	9500-13000	1.0-2.0

4.4 Influence of soil, plot, and chamber factors on CH_4 and N_2O emissions from rice experiment

To better understand the influence of soil, plot, and chamber factors on CH_4 and N_2O emissions from the rice experiment, we used a Principal Component Analysis

(PCA) (Fig. 13a, b). The GHG collection chamber had a negligible effect on the emission data variation, indicating that the collection method gave accurate and reliable results regarding the collection of N_2O and CH_4 emissions. There were some heterogeneities between plots in the experimental site since the experimental plot was positively correlated with silt, sand, and pH, and negatively correlated with clay and soil organic matter. CH_4 emissions were, as expected, positively correlated with both the soil organic matter parameters and water content since these factors have been known to affect CH_4 emissions (Yang & Chang 1998). Both silt and sand percentages negatively affected the methane emission rate, which was caused by reduced soil organic matter parameters when the sand and silt content increased (Ma et al. 2009). As expected, pH was also negatively correlated with CH_4 emissions since optimal methane production is near neutral pH (Bhattacharyya et al. 2013). In the rice cultivars, the N_2O emissions were not greatly affected by the different components of the soil, the distribution of the plots, or the water content; this could indicate that the soil was saturated during the irrigation period since it has been well described that soil water content affects N_2O emissions, resulting in increased N_2O emissions while drainage (Zou et al. 2005).

4.5 Displayed differences in yield components of koronivia grass cultivars

Koronivia grass is a widely used forage for cattle, where above-ground biomass production is an important production parameter (Durango Morales et al. 2021b). Forage can also increase or maintain high soil organic matter through its extensive root system (Damene et al. 2020), the roots can also affect soil nitrifier communities and inhibit nitrification and the production of nitrous oxide (Villegas et al. 2023). When biomass was compared between the two cultivars BH08 and CI67 (Fig. 14), no significant difference was found between the cultivars, which indicates similar growth behavior between cultivars and is supported by (Villegas et al. 2023). However, the dry mass yield presented in this report (Fig. 14d) was approximately 800 kg ha^{-1} and considerably low when compared to other experiments, presenting dry mass harvests of 1500-4000 kg ha^{-1} (Assis et al. 2013; Simon et al. 2020; Villegas et al. 2023). One reason explaining the low forage harvest is that only the first production cycle was sampled in this experiment, which was the establishment cycle of this perennial grass (Dereje et al. 2024), often grazed for several years before the soil is cultivated again (Fisher et al. 1994). For this reason, more cycles are needed to make more accurate evaluations and comparisons between the cultivars.

4.6 Effect of koronivia grass cultivar on N_2O and CH_4 emission profile

To our knowledge, the methane emission values presented in this report are the first recorded CH_4 emissions for Koronivia grass from field experiments. Comparisons to other forage grass species were made to contextualize the CH_4 emission values of Koronivia grass. Grassmann et al. (2020) performed field experiments in Brazil and presents methane emission values from Guinea grass, Palisade grass, and Ruzi grass, all showing negative emission values (indicating a net CH_4 uptake) when examining the cumulative emissions. However, Grassman reports positive CH_4 emissions from the forage grasses experiment during the first four months of the initial forage season, which aligns with the results presented in our trial (Fig. 15), where the CH_4 emission peak occurred within the initial months of the field trial.

When looking at the two cultivars (BH08 and CI67) used in this experiment, no significant difference was found when comparing cumulative CH_4 emissions (Fig. 15a). However, a tendency can be observed that indicates higher cumulative CH_4 emission from cultivar CI67. However, as mentioned, more production cycles are needed for greater understanding and to make more accurate evaluations of the emission profile of koronivia grass. These factors highlight the lack of research and knowledge of the CH_4 emissions from forage cultivation, especially from koronivia grass.

The CH_4 emission fluxes from both cultivars follow the same emission pattern to a large extent during the whole sampling period (Fig. 15b). However, during the first two days of sampling (DAT54 - DAT55), CH_4 emission decreased for cultivar BH08 and increased for cultivar CI67. One explanation could be soil disturbance due to chamber installation performed one day before the first sample event, causing potential root damage and potentially affecting emissions during the days after installation (Clough et al. 2020). However, the difference in emission was not perceived as significantly different in interval one, which covers the first days of sampling (Fig. 15c). When comparing the CH_4 emission variance (Fig. 15d), meaning how much the individual chambers within each cultivar differ; it was observed that the variation in emission rate was significantly higher for cultivar CI67 in interval one, with no clear explanation as to why. These findings indicate that more production cycles and on-farm experiments are needed to corroborate these findings and to create a strong foundation for comparisons in future research.

The N_2O emission fluxes from both cultivars (Fig. 16b) follow the same emission pattern with an emission peak after the fertilization event primarily caused by soil nitrifiers (Wang et al. 2021). When looking at the interval comparisons, N_2O emission was not significantly different in both intervals one and two (Fig. 16c), further supporting the probability of similar levels of nitrification inhibiting exudates from the plant roots during the whole sample period (Simon et al. 2020),

additionally supported by the equal size of variation between the cultivars, shown in (Fig. 16d).

4.7 Combined climatic impact of CH_4 and N_2O emissions and forage yield

When comparing the pGWP and YpGWP from the forage dry mass yield and combined cumulated methane and nitrous oxide emissions (Fig. 17a, b), a tendency for lower YpGWP can be observed for CI67 (Fig. 17b). However, it was not large enough to make a statistically significant difference. This is due to a lack of substantial difference in both the GHG emissions and yield components of the pGWP and YpGWP equation, further displaying the similarities between the cultivars in phenotypic and emission characteristics. Experiments comparing the GWP of koronivia grass were never done before, and therefore, there are no other reference values for comparison.

A closer reference could be Ghani et al. (2022), who presents net global warming potential (net GWP) and yield-based greenhouse gas intensity (GHGI) values for the two forage grasses, *Festuca arundinacea* Schreb. and *Bromus inermis* Leyss. The CO_2 emission amount included in the report presented by Ghani et al. (2022) was removed from the net GWP and GHGI for a fair comparison to the values presented in this report, where Net GWP is equivalent to pGWP, and YpGWP is equivalent to GHGI. The forage harvest and GHG emission values presented by Ghani et al. (2022) are shown in Table 5 and covers the first forage harvest of the grass species, which was sown nine months before the first sampling period; when comparing with the forage harvest presented in this work, we can see a three-fold higher harvest from Ghani et al. (2022). The reasons for the comparatively lower harvest of the koronivia grass were the differences in length of establishment time before sampling, along with poor establishment of the koronivia grass, which is reflected in the GWP components (Table 5).

Table 5. Comparison of grass dry weight harvest (ton ha^{-1}) and GWP components (kg CO_2 eq ha^{-1}).

source	forage harvest (kg/ha)	pGWP (kg CO_2 eq ha^{-1})	YpGWP (kg CO_2 eq kg^{-1} forage)
experimental values	776-860	125-133	0.14 - 0.17
Ghani et al. 2022	2381-2599	60-80	0.023-0.029

4.8 Influence of soil, plot, and chamber factors on CH_4 and N_2O emissions from koronivia grass experiment

To better understand the influence of soil, plot, and chamber factors on CH_4 and N_2O emissions from the koronivia grass experiment, a Principal Component Analysis (PCA) was used (Fig. 18a, b). The GHG collection chamber and precipitation had a negligible effect on the N_2O and CH_4 emission data variation, indicating that the precipitation amount did not affect soil water content enough to affect emission fluxes (Zou et al. 2005), and that the collection method gave accurate and reliable results regarding the collection of N_2O and CH_4 emissions. The CH_4 and N_2O emissions were not greatly affected by the soil composition, the distribution of the plots, or precipitation, indicating that these factors were not major contributors to differences in emissions seen from the different cultivars. There were some heterogeneities between plots in the experimental site since the experimental plot was positively correlated with sand content, pH, and bulk density and negatively correlated with organic matter parameters and clay content.

5. Conclusion

This study evaluated biomass, yield components, and emissions factors (CH_4 and N_2O) for two rice (Fedearroz 60 and HL23057) and two koronivia grass (CIAT 679 and BH08-1149) cultivars.

- Rice cultivar HL23 had higher grain yield and higher daily methane emission during the beginning of the sample period compared to cultivar FE60. Cultivar FE60 displayed a larger variance in daily CH_4 emission from flowering to the end of the sample period compared to cultivar HL23.
- Rice cultivation pGWP and YpGWP values presented in this work were 10-50-fold lower compared to literature, caused by the low cumulated methane emission values presented in this work.
- The koronivia grass cultivars BH08 and CI67 displayed similar biomass production; the dry-mass yield presented in this report was considerably lower than presented in the literature.

This study is the first report on methane emissions from a koronivia grass field experiment. Comparisons to other forage grass species were made to contextualize the net emission values of methane in koronivia grass and contrasted to the examples found in the literature, which presented a net CH_4- uptake. Koronivia grass cultivar CI67 displayed a significantly higher variance in daily CH_4 emissions during the beginning of the sample period compared to BH08, probably due soil disturbance caused during establishment.

This study provides insights into important characteristics of CH_4 and N_2O emissions and yield-related components of different rice and koronivia grass cultivars, and more production cycles will increase the understanding of the emission profile of forage grass and rice cultivation in Colombia.

The emissions factors presented will contribute to better quantify the effect of rice and koronivia grass cultivars on GHG emissions.

References

Abalos, D., van Groenigen, J.W. & De Deyn, G.B. (2018). What plant functional traits can reduce nitrous oxide emissions from intensively managed grasslands? *Global Change Biology*, 24 (1), e248–e258. https://doi.org/10.1111/gcb.13827

Albanito, F., Lebender, U., Cornulier, T., Sapkota, T.B., Brentrup, F., Stirling, C. & Hillier, J. (2017). Direct Nitrous Oxide Emissions From Tropical And Sub-Tropical Agricultural Systems - A Review And Modelling Of Emission Factors. *Scientific Reports*, 7 (1), 44235. https://doi.org/10.1038/srep44235

Alves, B.J.R., Smith, K.A., Flores, R.A., Cardoso, A.S., Oliveira, W.R.D., Jantalia, C.P., Urquiaga, S. & Boddey, R.M. (2012). Selection of the most suitable sampling time for static chambers for the estimation of daily mean N2O flux from soils. *Soil Biology and Biochemistry*, 46, 129–135. https://doi.org/10.1016/j.soilbio.2011.11.022

Arias-Navarro, C., Diaz-Pines, E., Kiese, R., Rosenstock, T.S., Rufino, M.C., Stern, D., Neufeldt, H., Verchot, L.V. & Butterbach-Bahl, K. (2013). *Gas pooling: a sampling technique to overcome spatial heterogeneity of soil carbon dioxide and nitrous oxide fluxes*. *CIFOR*. https://doi.org/10.1016/j.soilbio.2013.08.011

Assis, G.M.L. de, Valle, C.B. do, Andrade, C.M.S. de & Valentim, J.F. (2013). Selecting new Brachiaria humidicola hybrids for Western Brazilian Amazon. http://www.alice.cnptia.embrapa.br/handle/doc/970778 [2024-03-13]

Baruah, K.K., Gogoi, B. & Gogoi, P. (2010). Plant physiological and soil characteristics associated with methane and nitrous oxide emission from rice paddy. *Physiology and Molecular Biology of Plants*, 16 (1), 79–91. https://doi.org/10.1007/s12298-010-0010-1

Bates, D., Kliegl, R., Vasishth, S. & Baayen, H. (2018). Parsimonious Mixed Models. arXiv. https://doi.org/arXiv:1506.04967

Bayer, C., Costa, F. de S., Pedroso, G.M., Zschornack, T., Camargo, E.S., Lima, M.A. de, Frigheto, R.T.S., Gomes, J., Marcolin, E. & Macedo, V.R.M. (2014). Yield-scaled greenhouse gas emissions from flood irrigated rice under long-term conventional tillage and no-till systems in a Humid Subtropical climate. *Field Crops Research*, 162, 60–69. https://doi.org/10.1016/j.fcr.2014.03.015

Bhattacharyya, P., Roy, K.S., Neogi, S., Dash, P.K., Nayak, A.K., Mohanty, S., Baig, M.J., Sarkar, R.K. & Rao, K.S. (2013). Impact of elevated CO2 and temperature on soil C and N dynamics in relation to CH4 and N2O emissions from tropical flooded rice (Oryza sativa L.). *Science of The Total Environment*, 461–462, 601–611. https://doi.org/10.1016/j.scitotenv.2013.05.035

Camargo, E.S., Pedroso, G.M., Minamikawa, K., Shiratori, Y. & Bayer, C. (2018). Intercontinental comparison of greenhouse gas emissions from irrigated rice fields under feasible water management practices: Brazil and Japan. *Soil Science and Plant Nutrition*, 64 (1), 59–67. https://doi.org/10.1080/00380768.2017.1415660

Chen, Y., Li, S., Zhang, Y., Li, T., Ge, H., Xia, S., Gu, J., Zhang, H., Lü, B., Wu, X., Wang, Z., Yang, J., Zhang, J. & Liu, L. (2019). Rice root morphological and physiological traits interaction with rhizosphere soil and its effect on methane emissions in paddy fields. *Soil Biology and Biochemistry*, 129, 191–200. https://doi.org/10.1016/j.soilbio.2018.11.015

Clough, T.J., Rochette, P., Thomas, S.M., Pihlatie, M., Christiansen, J.R. & Thorman, R.E. (2020). Global Research Alliance N2O chamber methodology guidelines: Design considerations. *Journal of Environmental Quality*, 49 (5), 1081–1091. https://doi.org/10.1002/jeq2.20117

Costa, C., Villegas, D.M., Bastidas, M., Matiz-Rubio, N., Rao, I. & Arango, J. (2022). Soil carbon stocks and nitrous oxide emissions of pasture systems in Orinoquía region of Colombia: Potential for developing land-based greenhouse gas removal projects. *Frontiers in Climate*, 4, 916068. https://doi.org/10.3389/fclim.2022.916068

Damene, S., Bahir, A. & Villamor, G.B. (2020). The role of Chomo grass (Brachiaria humidicola) and exclosures in restoring soil organic matter, total nitrogen, and associated functions in degraded lands in Ethiopia. *Regional Environmental Change*, 20 (3), 92. https://doi.org/10.1007/s10113-020-01680-z

Dereje, F., Mengistu, A., Geleti, D., Feyissa, F., Diba, D., Pequeno, D. & Tesfaye, B. (2024). Calibration and evaluation of a CROPGRO Perennial Forage Model for Brachiaria humidicola yield simulation under future climate in subhumid environments of Ethiopia. *African Journal of Range & Forage Science*, 41 (4), 235–243. https://doi.org/10.2989/10220119.2024.2380699

Durango Morales, S.G., Barahona, R., Bolívar, D.M., Arango, J., Verchot, L. & Chirinda, N. (2021a). Apparent Nitrogen Recovery in Milk and Early Dry Season Nitrous Oxide Emission Factors for Urine Deposited by Dual-Purpose Cattle on Different Soil Types. *Frontiers in Sustainable Food Systems*, 4. https://doi.org/10.3389/fsufs.2020.602657

Fisher, M.J., Rao, I.M., Ayarza, M.A., Lascano, C.E., Sanz, J.I., Thomas, R.J. & Vera, R.R. (1994). Carbon storage by introduced deep-rooted grasses in the South American savannas. *Nature*, 371 (6494), 236–238. https://doi.org/10.1038/371236a0

Ghani, M.U., Kamran, M., Ahmad, I., Arshad, A., Zhang, C., Zhu, W., Lou, S. & Hou, F. (2022). Alfalfa-grass mixtures reduce greenhouse gas emissions and net global warming potential while maintaining yield advantages over monocultures. *Science of The Total Environment*, 849, 157765. https://doi.org/10.1016/j.scitotenv.2022.157765

Google Earth 10.48.0.4 (2023) *Palmira*, Valle del cauca, 3°30'16“N 76°21'20“W, elevation 968 [online]. Available from https://earth.google.com/web/@3.50406187,-76.35514596,968.20777602a,821.95536461d,35y,0h,0t,0r/data=OgMKATA [accessed 22 February 2024]

Grassmann, C.S., Mariano, E., Rocha, K.F., Gilli, B.R. & Rosolem, C.A. (2020). Effect of tropical grass and nitrogen fertilization on nitrous oxide, methane, and ammonia emissions of maize-based rotation systems. *Atmospheric Environment*, 234, 117571. https://doi.org/10.1016/j.atmosenv.2020.117571

Horrocks, C.A., Arango, J., Arevalo, A., Nuñez, J., Cardoso, J.A. & Dungait, J.A.J. (2019). Smart forage selection could significantly improve soil health in the tropics. *Science of The Total Environment*, 688, 609–621. https://doi.org/10.1016/j.scitotenv.2019.06.152

Hussain, S., Peng, S., Fahad, S., Khaliq, A., Huang, J., Cui, K. & Nie, L. (2015). Rice management interventions to mitigate greenhouse gas emissions: a

review. *Environmental Science and Pollution Research*, 22 (5), 3342–3360. https://doi.org/10.1007/s11356-014-3760-4

Jaffar, M.K., Sa'adan, N.S.M. & Chua, L.S. (2024). Determination of Available Phosphorus In Soil Using ICP-OES And UV- VIS Spectrophotometer: A Comparison. 28

Kelliher, F.M., Cox, N., van der Weerden, T.J., de Klein, C.A.M., Luo, J., Cameron, K.C., Di, H.J., Giltrap, D. & Rys, G. (2014). Statistical analysis of nitrous oxide emission factors from pastoral agriculture field trials conducted in New Zealand. *Environmental Pollution*, 186, 63–66. https://doi.org/10.1016/j.envpol.2013.11.025

Kim, W.-J., Bui, L.T., Chun, J.-B., McClung, A.M. & Barnaby, J.Y. (2018). Correlation between Methane (CH4) Emissions and Root Aerenchyma of Rice Varieties. *Plant Breeding and Biotechnology*, 6 (4), 381–390. https://doi.org/10.9787/PBB.2018.6.4.381

L, J.C.G., Posada-Suárez, H. & Läderach, P. (2014). Recommendations for the Regionalizing of Coffee Cultivation in Colombia: A Methodological Proposal Based on Agro-Climatic Indices. *PLOS ONE*, 9 (12), e113510. https://doi.org/10.1371/journal.pone.0113510

Li, S., Chen, L., Han, X., Yang, K., Liu, K., Wang, J., Chen, Y. & Liu, L. (2022). Rice Cultivar Renewal Reduces Methane Emissions by Improving Root Traits and Optimizing Photosynthetic Carbon Allocation. *Agriculture*, 12 (12), 2134. https://doi.org/10.3390/agriculture12122134

Liang, C. (2020). Application of Atomic Absorption Spectrometry in Soil Environmental Monitoring. *Science and Technology*, 2 (15), 46–50

Loaiza, S., Verchot, L., Valencia, D., Guzmán, P., Amezquita, N., Garcés, G., Puentes, O., Trujillo, C., Chirinda, N. & Pittelkow, C.M. (2024). Evaluating greenhouse gas mitigation through alternate wetting and drying irrigation in Colombian rice production. *Agriculture, Ecosystems & Environment*, 360, 108787. https://doi.org/10.1016/j.agee.2023.108787

Ma, K., Qiu, Q. & Lu, Y. (2009). Microbial mechanism for rice variety control on methane emission from rice field soil: METHANE EMISSION FROM PADDY FIELD. *Global Change Biology*, no-no. https://doi.org/10.1111/j.1365-2486.2009.02145.x

Malyan, S.K., Bhatia, A., Kumar, A., Gupta, D.K., Singh, R., Kumar, S.S., Tomer, R., Kumar, O. & Jain, N. (2016). Methane production, oxidation and mitigation: A mechanistic understanding and comprehensive evaluation of influencing factors. *Science of The Total Environment*, 572, 874–896. https://doi.org/10.1016/j.scitotenv.2016.07.182

Moterle, D.F., Silva, L.S. da, Moro, V.J., Bayer, C., Zschornack, T., Avila, L.A. de & Bundt, Â. da C. (2013). Methane efflux in rice paddy field under different irrigation managements. *Revista Brasileira de Ciência do Solo*, 37, 431–437. https://doi.org/10.1590/S0100-06832013000200014

Mukamuhirwa, A. (2019). *Grain Yield and Quality Traits of Rice (Oryza sativa L.) Cultivars under Intermittent Drought and Contrasting Temperatures*

Nikolaisen, M., Cornulier, T., Hillier, J., Smith, P., Albanito, F. & Nayak, D. (2023). Methane emissions from rice paddies globally: A quantitative statistical review of controlling variables and modelling of emission factors. *Journal of Cleaner Production*, 409, 137245. https://doi.org/10.1016/j.jclepro.2023.137245

Oo, A.Z., Sudo, S., Inubushi, K., Mano, M., Yamamoto, A., Ono, K., Osawa, T., Hayashida, S., Patra, P.K., Terao, Y., Elayakumar, P., Vanitha, K., Umamageswari, C., Jothimani, P. & Ravi, V. (2018). Methane and nitrous oxide emissions from conventional and modified rice cultivation systems in South India. *Agriculture, Ecosystems & Environment*, 252, 148–158. https://doi.org/10.1016/j.agee.2017.10.014

Owino, C.N., Kitaka, N., Kipkemboi, J. & Ondiek, R.A. (2020). Assessment of Greenhouse Gases Emission in Smallholder Rice Paddies Converted From Anyiko Wetland, Kenya. *Frontiers in Environmental Science*, 8. https://doi.org/10.3389/fenvs.2020.00080

Pepper, I.L. & Gentry, T.J. (2015). Chapter 4 - Earth Environments. In: Pepper, I.L., Gerba, C.P., & Gentry, T.J. (eds) *Environmental Microbiology (Third Edition)*. Academic Press. 59–88. https://doi.org/10.1016/B978-0-12-394626-3.00004-1

Rakshit, A., Singh, S.K., Abhilash, P.C. & Biswas, A. (eds) (2021). *Soil Science: Fundamentals to Recent Advances*. Springer Singapore. https://doi.org/10.1007/978-981-16-0917-6

Rodriguez Baquero, A.K. (2016). *Efectos de Siembra Escalonada de Algunos Hibridos y Variedades de Arroz(Oryza Sativa) sobre Componentes Vegetativos y Componentes de Rendimiento en Santa Rosa Villavicencio./*. Villavicencio, Universidad de los Llanos, 2016. https://repositorio.unillanos.edu.co/handle/001/342 [2024-09-01]

Ruxton, G.D. (2006). The unequal variance t-test is an underused alternative to Student's t-test and the Mann–Whitney U test. *Behavioral Ecology*, 17 (4), 688–690. https://doi.org/10.1093/beheco/ark016

Sainani, K.L. (2012). Dealing With Non-normal Data. *PM&R*, 4 (12), 1001–1005. https://doi.org/10.1016/j.pmrj.2012.10.013

Simon, P.L., Dieckow, J., Zanatta, J.A., Ramalho, B., Ribeiro, R.H., van der Weerden, T. & de Klein, C.A.M. (2020). Does Brachiaria humidicola and dicyandiamide reduce nitrous oxide and ammonia emissions from cattle urine patches in the subtropics? *Science of The Total Environment*, 720, 137692. https://doi.org/10.1016/j.scitotenv.2020.137692

Smart, A., Schacht, W. & Moser, L. (2001). Predicting Leaf/Stem Ratio and Nutritive Value in Grazed and Nongrazed Big Bluestem. *Agronomy Journal - AGRON J*, 93. https://doi.org/10.2134/agronj2001.1243

Smith, K.A. & Dobbie, K.E. (2002). The impact of sampling frequency and sampling times on chamber-based measurements of N2O emissions from fertilized soils. https://onlinelibrary.wiley.com/doi/10.1046/j.1354-1013.2001.00450.x [2025-03-10]

Solomon, S., Intergovernmental Panel on Climate Change, & Intergovernmental Panel on Climate Change (eds) (2007). *Climate change 2007: the physical science basis: contribution of Working Group I to the Fourth Assessment Report of the Intergovernmental Panel on Climate Change*. Cambridge University Press.

Stoffel, M.A., Nakagawa, S. & Schielzeth, H. (2017). rptR: repeatability estimation and variance decomposition by generalized linear mixed-effects models. *Methods in Ecology and Evolution*, 8 (11), 1639–1644. https://doi.org/10.1111/2041-210X.12797

Subbarao, G.V., Nakahara, K., Hurtado, M.P., Ono, H., Moreta, D.E., Salcedo, A.F., Yoshihashi, A.T., Ishikawa, T., Ishitani, M., Ohnishi-Kameyama, M., Yoshida, M., Rondon, M., Rao, I.M., Lascano, C.E., Berry, W.L. & Ito, O. (2009). Evidence for biological nitrification inhibition in Brachiaria pastures. *Proceedings of the National Academy of Sciences*, 106 (41), 17302–17307. https://doi.org/10.1073/pnas.0903694106

Vik, P. (2013). *Regression, ANOVA, and the General Linear Model: A Statistics Primer*. SAGE Publications.

Villegas, D.M., Arévalo, A., Sotelo, M., Nuñez, J., Moreta, D., Rao, I., Ishitani, M., Subbarao, G.V. & Arango, J. (2023). Phenotyping of Urochloa humidicola grass hybrids for agronomic and environmental performance in the Piedmont region of the Orinoquian savannas of Colombia. *Grass and Forage Science*, 78 (1), 119–128. https://doi.org/10.1111/gfs.12582

Wang, C., Amon, B., Schulz, K. & Mehdi, B. (2021). Factors That Influence Nitrous Oxide Emissions from Agricultural Soils as Well as Their Representation in Simulation Models: A Review. *Agronomy*, 11 (4), 770. https://doi.org/10.3390/agronomy11040770

Wassmann, R. & Aulakh, M.S. (2000). The role of rice plants in regulating mechanisms of methane missions. *Biology and Fertility of Soils*, 31 (1), 20–29. https://doi.org/10.1007/s003740050619

Westberg, D Stackhouse, P.W, Hoell, J.M, Chandler, W.S, & and Zhang, T (2015). Prediction of Worldwide Energy Resource (POWER)-Agroclimatology methodology-(1.0 latitude by 1.0 longitude spatial resolution). Prediction of Worldwide Energy Resource (POWER)-Agroclimatology methodology-(1.0 latitude by 1.0 longitude spatial resolution)

Xie, L., Liu, D., Müller, C., Jansen-Willems, A., Chen, Z., Niu, Y., Zaman, M., Meng, L. & Ding, W. (2022). Brachiaria humidicola Cultivation Enhances Soil Nitrous Oxide Emissions from Tropical Grassland by Promoting the Denitrification Potential: A 15N Tracing Study. *Agriculture*, 12 (11), 1940. https://doi.org/10.3390/agriculture12111940

Yagi, K., Minami, K. & Ogawa, Y. (1998). Effects of water percolation on methane emission from rice paddies: a lysimeter experiment. *Plant and Soil*, 198, 193–200. https://doi.org/10.1023/A:1004379914540

Yang, S.-S. & Chang, H.-L. (1998). Effect of environmental conditions on methane production and emission from paddy soil. *Agriculture, Ecosystems & Environment*, 69 (1), 69–80. https://doi.org/10.1016/S0167-8809(98)00098-X

Zou, J., Huang, Y., Jiang, J., Zheng, X. & Sass, R.L. (2005). A 3-year field measurement of methane and nitrous oxide emissions from rice paddies in China: Effects of water regime, crop residue, and fertilizer application: EFFECTS OF AGRICULTURAL MANAGEMENT ON CHINA. http://doi.wiley.com/10.1029/2004GB002401 [2023-01-18]

Zschornack, T., da Rosa, C.M., Pedroso, G.M., Marcolin, E., da Silva, P.R.F. & Bayer, C. (2016). Mitigation of yield-scaled greenhouse gas emissions in subtropical paddy rice under alternative irrigation systems. *Nutrient Cycling in Agroecosystems*, 105 (1), 61–73. https://doi.org/10.1007/s10705-016-9775-0

Popular science summary

Agriculture plays an important role in feeding the world, but it produces a lot of greenhouse gas emissions which heats up the planet and has a direct impact on agriculture because of more unstable climate. In Colombia, flood-irrigated rice cultivation and forage grazing are two important agricultural activities that release large amounts of planet-heating methane (CH_4) and nitrous oxide (N_2O) gases into the atmosphere, which means that it is important to understand how the emissions are created and how we can reduce them, to reduce climate change.

In this study, we focused on the methane and nitrous oxide emissions from two rice cultivars and two koronivia grass cultivars, a forage grass with a natural ability to reduce N_2O emissions through a special compound that the roots send out called brachialactone.

We did the field experiments at the CIAT Research Center in Colombia, where we measured greenhouse gas emissions and crop yields (since a larger yield can allow for higher emissions). We saw that the rice cultivar, HL23 had the highest grain yield production but also released the most methane early in the growing period, the other rice cultivar FE60 showed more variation in methane emissions later in the season. In this study, we investigated for the first time methane emission from koronivia grass in field conditions, where we could reveal that the koronivia grass cultivar CI67, emitted more methane at the beginning of the sampling period.

Understanding how different plant cultivars affect greenhouse gas emissions is very important for the development of more environmentally sustainable farming practices in tropical regions like Colombia. This research also provides valuable data that can help in the development of crops and gives insights to policymakers who want to reduce the environmental impact of agriculture in tropical regions.

Acknowledgments

I want to thank my primary supervisor, Marcos Lana, and my assistant supervisor, Miguel Antonio Romero Sanchez, at CIAT in Colombia for the technical support and guidance. I thank my wonderful girlfriend, and my parents for supporting and helping me when I felt like it was difficult to continue. I would like to express my sincere gratitude for the financial support provided by Minor Field Studies (MFS), managed by the SLU mobility team and funded by the Swedish International Development Cooperation Agency (SIDA).

Appendix 1

Table 6. Soil chemical analysis data, taken from the plots of the research site at five soil depths (0-5, 5-10, 10-30, 30-60, and 60-100 cm).

sample	Description	pH (Un)	C Oxid (g/kg)	SOM (g/kg)	P-BrayII	Ca	Mg	K	Al	Na	CIC	CIC	Fe	Mn	Cu	Zn	B	S
						cmol/kg							mg/kg					
1	SCP1-S-MD-0-5CM	7.95	15.27	34.67	50.32	18.11	10.13	0.77	NA	0.20	NA	27.50	2.28	78.42	0.42	3.04	1.29	14.96
2	SCP1-S-MD-5-10CM	8.21	14.53	32.99	49.25	42.48	9.46	0.76	NA	0.23	NA	27.40	4.54	75.10	0.61	2.90	1.38	15.53
3	SCP1-S-MD-10-30CM	8.18	15.17	34.43	26.42	36.76	12.73	0.62	NA	0.35	NA	29.80	1.37	55.04	0.17	1.26	0.89	19.45
4	SCP1-S-MD-30-60CM	8.37	8.16	18.52	9.42	17.77	20.11	0.49	NA	0.43	NA	27.20	1.98	47.60	0.04	0.09	0.31	19.09
5	SCP1-S-MD-60-100CM	8.33	7.31	16.59	5.54	13.97	16.44	0.41	NA	0.40	NA	23.20	19.47	78.90	0.09	0.35	0.17	16.33
6	SCP2-S-MD-0-5CM	8.03	13.12	29.79	59.61	19.49	8.60	0.80	NA	0.19	NA	29.00	4.08	54.57	0.71	3.71	1.20	15.03
7	SCP2-S-MD-5-10CM	8.00	15.68	35.60	58.93	44.94	9.12	0.76	NA	0.20	NA	28.40	5.87	64.38	0.83	4.07	1.34	15.43
8	SCP2-S-MD-10-30CM	8.15	14.39	32.67	30.41	19.66	11.08	0.60	NA	0.30	NA	28.00	2.58	44.42	0.43	1.95	0.98	17.77
9	SCP2-S-MD-30-60CM	8.42	7.49	16.99	9.88	16.55	13.74	0.47	NA	0.37	NA	27.00	0.04	24.10	0.05	0.03	0.48	15.19
10	SCP2-S-MD-60-100CM	8.43	5.54	12.58	7.41	12.21	13.45	0.36	NA	0.36	NA	22.60	5.08	55.92	0.23	0.25	0.16	17.53
11	SCP3-S-MD-0-5CM	7.64	21.14	48.01	78.08	14.36	5.31	0.86	NA	0.20	NA	26.95	5.54	78.34	0.77	4.72	1.48	18.89
12	SCP3-S-MD-5-10CM	7.81	19.54	44.35	73.42	10.89	3.60	0.83	NA	0.33	NA	26.66	5.87	83.02	0.81	5.31	1.69	15.49
13	SCP3-S-MD-10-30CM	8.00	12.35	28.03	42.04	11.59	5.49	0.65	NA	0.29	NA	26.86	3.31	63.80	0.53	3.77	1.13	14.71
14	SCP3-S-MD-30-60CM	8.08	9.99	22.68	14.65	12.73	9.72	0.53	NA	0.70	NA	27.24	0.00	20.03	0.03	0.20	0.77	15.15
15	SCP3-S-MD-60-100CM	8.25	3.95	8.97	3.42	9.86	12.16	0.43	NA	0.48	NA	26.66	0.09	20.61	0.02	0.08	0.25	23.28
16	SCP4-S-MD-0-5CM	7.86	19.96	45.31	87.66	12.81	4.23	0.96	NA	0.20	NA	26.66	3.77	83.15	0.67	6.86	1.58	15.93
17	SCP4-S-MD-5-10CM	7.87	19.37	43.99	91.11	14.07	5.11	1.03	NA	0.22	NA	26.47	3.02	88.18	0.67	6.72	0.62	17.27
18	SCP4-S-MD-10-30CM	7.93	18.88	42.86	66.77	14.88	5.68	0.69	NA	0.27	NA	27.05	2.57	87.42	0.69	6.19	1.06	18.27
19	SCP4-S-MD-30-60CM	7.99	13.35	30.30	19.66	13.11	6.87	0.52	NA	0.36	NA	26.66	0.15	26.06	0.26	0.68	0.64	15.37
20	SCP4-S-MD-60-100CM	8.24	10.09	22.91	5.35	12.89	12.58	0.45	NA	0.53	NA	24.74	0.00	17.79	0.08	0.00	0.25	22.01
21	SCP5-S-MD-0-5CM	7.82	16.69	37.89	92.93	14.53	4.97	0.94	NA	0.20	NA	26.86	1.82	61.23	0.68	6.43	1.46	15.13
22	SCP5-S-MD-5-10CM	7.77	18.87	42.85	90.71	13.60	4.76	0.94	NA	0.21	NA	25.90	2.05	70.98	0.75	7.13	1.39	16.63
23	SCP5-S-MD-10-30CM	7.76	20.22	45.91	67.56	12.49	4.47	0.72	NA	0.23	NA	27.05	6.10	60.65	0.99	6.03	1.23	15.83
24	SCP5-S-MD-30-60CM	7.97	12.28	27.87	32.24	13.39	7.02	0.58	NA	0.33	NA	27.24	0.66	48.17	0.36	2.72	0.69	18.53
25	SCP5-S-MD-60-100CM	8.20	9.43	21.41	4.59	11.66	10.72	0.50	NA	0.43	NA	26.86	0.00	14.53	0.06	0.00	0.44	21.99
26	SCP6-S-MD-0-5CM	7.69	21.23	48.20	89.45	12.30	4.86	0.93	NA	0.18	NA	25.87	2.26	75.97	0.59	6.01	1.65	15.21
27	SCP6-S-MD-5-10CM	7.84	21.08	47.85	91.57	13.98	5.64	0.97	NA	0.19	NA	24.94	2.11	77.19	0.51	6.04	1.69	16.77
28	SCP6-S-MD-10-30CM	7.84	17.84	40.50	70.66	14.40	6.47	0.78	NA	0.25	NA	24.36	2.14	71.61	0.42	4.77	1.50	16.31
29	SCP6-S-MD-30-60CM	8.07	14.04	31.89	36.06	14.66	8.14	0.65	NA	0.33	NA	23.02	2.93	39.89	0.30	1.48	0.96	18.79
30	SCP6-S-MD-60-100CM	8.17	10.69	24.27	12.02	11.58	9.52	0.54	NA	0.36	NA	23.68	0.74	42.43	0.10	0.33	0.41	19.41
31	SCP7-S-MD-0-5CM	7.44	17.14	38.92	82.78	14.89	5.90	0.98	NA	0.20	NA	27.40	1.34	87.33	0.44	5.79	1.37	20.17
32	SCP7-S-MD-5-10CM	7.86	21.96	49.86	78.23	14.50	6.32	0.88	NA	0.23	NA	27.60	1.93	68.50	0.46	5.57	1.64	20.51
33	SCP7-S-MD-10-30CM	7.78	18.14	41.19	69.44	14.84	6.63	0.73	NA	0.26	NA	27.00	2.14	86.34	0.50	6.09	1.21	19.05
34	SCP7-S-MD-30-60CM	8.52	15.86	36.02	28.35	16.19	11.04	0.58	NA	0.38	NA	27.60	0.92	70.56	0.16	1.87	0.54	20.51
35	SCP7-S-MD-60-100CM	8.31	7.55	17.13	6.45	10.47	13.31	0.44	NA	0.52	NA	27.00	0.00	18.16	0.04	0.00	0.26	23.30
36	SCP8-S-MD-0-5CM	8.01	20.16	45.78	77.28	13.42	5.74	0.88	NA	0.19	NA	28.40	2.65	100.53	0.66	6.71	1.50	17.55
37	SCP8-S-MD-5-10CM	8.21	18.97	43.08	84.77	14.18	6.01	0.89	NA	0.21	NA	27.40	1.80	100.48	0.57	7.20	0.87	25.02
38	SCP8-S-MD-10-30CM	8.11	15.92	36.14	53.79	13.37	6.72	0.62	NA	0.25	NA	27.20	2.93	76.75	0.85	6.10	1.02	20.15
39	SCP8-S-MD-30-60CM	8.15	11.45	26.00	16.12	11.10	9.42	0.43	NA	0.46	NA	27.20	0.00	31.55	0.03	0.15	0.56	20.80
40	SCP8-S-MD-60-100CM	8.33	9.45	21.46	5.77	10.23	12.05	0.35	NA	0.49	NA	25.60	0.00	38.63	0.05	0.03	0.27	24.27
41	SCP9-S-MD-0-5CM	8.05	20.01	45.43	84.76	14.01	5.94	0.96	NA	0.19	NA	28.20	2.15	95.70	0.57	6.64	0.86	19.94
42	SCP9-S-MD-5-10CM	7.93	20.30	46.10	80.25	13.73	5.46	0.83	NA	0.21	NA	27.20	2.37	85.26	0.68	6.92	0.72	19.19
43	SCP9-S-MD-10-30CM	7.94	17.28	39.23	61.84	14.25	6.36	0.67	NA	0.24	NA	27.40	2.80	83.41	1.40	8.21	1.20	17.63
44	SCP9-S-MD-30-60CM	8.24	13.01	29.53	18.95	13.45	9.51	0.46	NA	0.36	NA	27.00	0.34	41.03	0.13	0.95	1.44	22.82
45	SCP9-S-MD-60-100CM	8.45	9.54	21.65	4.59	10.36	11.76	0.35	NA	0.43	NA	26.60	0.00	50.32	0.04	0.15	0.55	21.98
46	SCP10-S-MD-0-5CM	8.13	18.27	41.49	51.33	13.30	6.49	0.77	NA	0.27	NA	28.40	2.69	64.48	0.54	3.15	1.43	20.46
47	SCP10-S-MD-5-10CM	8.12	18.57	42.17	66.32	13.36	5.74	0.82	NA	0.21	NA	28.20	2.88	75.83	0.73	4.24	1.59	20.51
48	SCP10-S-MD-10-30CM	8.14	14.73	33.45	47.63	16.24	8.46	0.61	NA	0.28	NA	27.60	2.92	60.00	0.64	3.15	1.16	21.42
49	SCP10-S-MD-30-60CM	8.21	10.62	24.11	10.19	14.88	12.88	0.43	NA	0.42	NA	28.40	0.00	29.51	0.03	0.06	0.26	22.15
50	SCP10-S-MD-60-100CM	8.34	6.30	14.30	3.03	10.90	15.12	0.33	NA	0.55	NA	26.00	0.07	50.83	0.03	0.11	0.33	23.13
51	SCP11-S-MD-0-5CM	7.87	20.27	46.02	56.97	16.50	7.02	0.73	NA	0.20	NA	28.60	3.50	65.71	0.71	3.07	0.60	17.72
52	SCP11-S-MD-5-10CM	7.96	19.69	44.71	58.50	18.15	7.35	0.77	NA	0.22	NA	29.20	5.41	65.47	0.74	2.81	0.60	26.13
53	SCP11-S-MD-10-30CM	7.92	18.94	43.00	36.23	16.40	7.40	0.66	NA	0.29	NA	29.00	4.39	68.53	0.65	2.55	0.68	22.38
54	SCP11-S-MD-30-60CM	8.26	7.24	16.44	7.53	15.14	12.02	0.46	NA	0.45	NA	27.80	0.03	31.08	0.05	0.00	0.27	26.50
55	SCP11-S-MD-60-100CM	8.50	6.97	15.82	3.64	11.52	14.33	0.37	NA	0.53	NA	25.20	0.88	65.13	0.17	0.29	0.02	23.61

56	SCP12-S-MD-0-5CM	8.00	21.94	49.81	61.93	16.70	6.77	0.82	NA	0.19	NA	27.80	0.91	84.04	0.39	3.17	0.83	22.32
57	SCP12-S-MD-5-10CM	7.92	19.29	43.79	61.38	16.35	6.68	0.78	NA	0.21	NA	29.20	1.20	72.58	0.38	2.99	0.78	21.84
58	SCP12-S-MD-10-30C	8.00	16.14	36.65	34.57	18.89	9.51	0.61	NA	0.30	NA	28.00	0.17	65.58	0.14	1.25	0.57	19.44
59	SCP12-S-MD-30-60C	8.21	9.91	22.50	7.18	14.42	13.12	0.47	NA	0.44	NA	24.80	0.00	29.17	0.04	0.00	0.07	26.63
60	SCP12-S-MD-60-100	8.27	8.56	19.44	8.13	12.11	13.95	0.44	NA	0.48	NA	24.60	0.64	79.52	0.07	0.18	0.00	22.24
61	SCP13-S-MD-0-5CM	8.11	18.58	42.18	63.05	14.47	5.66	0.74	NA	0.46	NA	26.60	0.31	57.19	0.12	1.31	1.41	20.51
62	SCP13-S-MD-5-10CM	8.24	20.09	45.62	61.98	15.58	5.97	0.73	NA	0.53	NA	26.40	0.39	55.13	0.08	1.29	0.89	20.86
63	SCP13-S-MD-10-30C	8.26	12.27	27.86	42.35	15.88	7.96	0.59	NA	0.66	NA	25.60	0.39	61.70	0.07	0.84	0.82	23.50
64	SCP13-S-MD-30-60C	8.37	9.18	20.85	18.37	12.93	12.97	0.52	NA	1.43	NA	26.40	2.96	53.53	0.09	0.39	0.82	23.96
65	SCP13-S-MD-60-100	8.56	8.95	20.31	13.94	10.02	13.35	0.40	NA	6.48	NA	24.60	0.80	91.67	0.07	0.46	0.81	25.65
66	SCP14-S-MD-0-5CM	8.12	16.75	38.04	66.39	17.57	6.65	0.67	NA	0.56	NA	25.50	0.46	52.03	0.09	1.52	1.50	21.96
67	SCP14-S-MD-5-10CM	8.20	17.51	39.76	64.76	16.32	6.27	0.56	NA	0.50	NA	25.80	0.40	59.19	0.11	1.45	1.35	22.59
68	SCP14-S-MD-10-30C	8.22	14.19	32.21	37.38	16.32	9.46	0.53	NA	1.13	NA	24.80	0.55	50.83	0.07	0.87	1.12	23.88
69	SCP14-S-MD-30-60C	8.62	9.72	22.07	16.46	11.07	12.91	0.35	NA	4.32	NA	23.40	0.23	27.29	0.00	0.06	0.99	27.88
70	SCP14-S-MD-60-100	8.68	7.16	16.26	7.30	10.31	15.64	0.34	NA	5.14	NA	22.20	3.21	75.99	0.05	0.23	0.73	31.02
71	SCP15-S-MD-0-5CM	7.93	17.62	40.01	71.70	16.79	6.28	0.65	NA	0.19	NA	17.60	2.21	54.38	0.33	2.14	0.85	38.27
72	SCP15-S-MD-5-10CM	8.03	17.63	40.04	71.28	35.56	7.58	0.92	NA	0.32	NA	27.00	2.65	65.82	0.32	2.20	0.99	15.70
73	SCP15-S-MD-10-30C	8.11	15.42	35.02	45.05	32.49	10.80	0.68	NA	0.58	NA	26.20	2.79	48.33	0.29	1.54	0.53	24.18
74	SCP15-S-MD-30-60C	8.47	9.17	20.82	14.66	13.42	14.62	0.54	NA	1.37	NA	25.40	5.29	41.35	0.03	0.21	0.25	31.22
75	SCP15-S-MD-60-100	8.60	7.96	18.07	7.43	10.27	15.39	0.43	NA	1.62	NA	22.00	15.75	90.88	0.36	0.54	0.17	28.26
76	SCP16-S-MD-0-5CM	8.09	18.71	42.47	80.41	15.77	5.09	0.81	NA	0.19	NA	25.60	2.15	47.58	0.47	2.81	0.85	14.88
77	SCP16-S-MD-5-10CM	8.15	18.63	42.29	83.79	17.08	5.34	0.82	NA	0.15	NA	26.00	3.68	56.70	0.38	2.78	0.89	44.01
78	SCP16-S-MD-10-30C	8.10	15.17	34.45	52.75	15.28	6.82	0.71	NA	0.27	NA	25.60	1.18	37.02	0.22	1.78	0.69	18.60
79	SCP16-S-MD-30-60C	8.26	11.28	25.60	19.93	13.18	8.82	0.51	NA	3.77	NA	22.60	0.08	29.78	0.03	0.15	0.37	16.77
80	SCP16-S-MD-60-100	8.44	7.84	17.79	10.57	11.67	13.18	0.52	NA	0.55	NA	22.60	2.09	56.19	0.13	0.48	0.30	18.44
81	SCP17-S-MD-0-5CM	8.16	21.32	48.40	83.31	18.86	5.44	0.79	NA	0.14	NA	22.40	1.60	49.11	0.33	2.62	0.91	14.94
82	SCP17-S-MD-5-10CM	8.01	19.44	44.14	81.78	17.76	5.19	0.86	NA	0.17	NA	26.20	1.44	50.28	0.25	2.51	0.90	16.90
83	SCP17-S-MD-10-30C	8.11	16.60	37.68	68.00	18.97	6.57	0.74	NA	0.22	NA	25.40	0.54	49.75	0.09	1.86	0.68	38.45
84	SCP17-S-MD-30-60C	8.23	12.40	28.16	28.44	16.44	8.55	0.59	NA	0.29	NA	24.60	1.25	51.60	0.09	0.90	0.39	15.02
85	SCP17-S-MD-60-100	8.33	7.91	17.96	7.19	13.87	16.18	0.49	NA	0.46	NA	26.40	1.17	50.43	0.13	0.35	0.16	23.69
86	SCP18-S-MD-0-5CM	7.99	19.82	44.99	98.05	17.46	5.18	0.75	NA	0.15	NA	25.20	2.33	47.25	0.27	1.80	1.29	17.58
87	SCP18-S-MD-5-10CM	8.01	19.73	44.79	88.71	17.72	5.94	0.66	NA	0.16	NA	25.20	2.32	50.63	0.26	1.40	0.94	23.61
88	SCP18-S-MD-10-30C	8.08	18.90	42.91	82.28	17.52	5.39	0.67	NA	0.16	NA	22.20	0.28	52.98	0.11	1.03	0.54	18.32
89	SCP18-S-MD-30-60C	8.24	11.92	27.06	34.55	14.29	8.72	0.37	NA	0.29	NA	20.20	0.17	30.95	0.07	0.22	0.22	20.21
90	SCP18-S-MD-60-100	8.34	7.96	18.06	13.12	16.42	14.15	0.48	NA	0.47	NA	27.20	0.06	31.85	0.00	0.02	0.00	25.32
91	SCP19-S-MD-0-5CM	8.20	19.65	44.62	87.43	48.35	5.68	0.88	NA	0.16	NA	22.80	5.30	52.01	0.23	1.66	1.70	16.09
92	SCP19-S-MD-5-10CM	8.10	19.81	44.99	86.47	102.29	5.85	0.86	NA	0.17	NA	22.40	8.00	43.33	0.27	1.96	1.79	20.09
93	SCP19-S-MD-10-30C	8.13	14.94	33.91	74.09	18.67	5.52	0.61	NA	0.22	NA	21.80	2.77	34.84	0.17	1.48	1.15	18.95
94	SCP19-S-MD-30-60C	8.43	12.13	27.53	82.96	19.05	6.88	0.49	NA	0.32	NA	20.60	7.17	40.17	0.20	1.10	0.83	19.07
95	SCP19-S-MD-60-100	8.42	9.25	21.01	90.75	14.03	7.76	0.40	NA	0.49	NA	19.60	14.77	31.71	0.59	0.68	0.57	20.53
96	SCP20-S-MD-0-5CM	8.13	17.36	39.40	90.27	19.52	5.21	0.79	NA	0.14	NA	21.80	5.15	40.01	0.32	1.61	1.45	22.43
97	SCP20-S-MD-5-10CM	8.26	16.31	37.04	86.36	17.54	4.91	0.78	NA	0.17	NA	20.90	3.02	37.19	0.21	1.37	1.52	17.55
98	SCP20-S-MD-10-30C	8.25	15.61	35.44	68.83	19.53	6.00	0.63	NA	0.22	NA	21.08	2.08	30.64	0.14	1.12	1.16	17.67
99	SCP20-S-MD-30-60C	8.44	12.71	28.86	51.62	18.64	6.47	0.45	NA	0.26	NA	19.44	2.68	30.86	0.13	0.81	1.14	15.79
100	SCP20-S-MD-60-10C	8.68	6.77	15.37	42.98	15.88	7.85	0.35	NA	0.29	NA	17.25	15.11	42.54	0.54	0.68	0.36	14.77
101	SCP21-S-MD-0-5CM	8.14	19.84	45.04	88.18	16.68	4.18	0.67	NA	0.14	NA	22.80	0.35	30.29	0.06	0.81	0.59	21.53
102	SCP21-S-MD-5-10CM	8.13	17.74	40.28	89.36	17.15	4.30	0.76	NA	0.16	NA	20.80	1.01	29.40	0.14	1.92	0.58	16.44
103	SCP21-S-MD-10-30C	8.25	14.45	32.81	62.51	16.17	4.46	0.48	NA	0.21	NA	21.20	0.04	29.29	0.06	0.84	0.39	45.02
104	SCP21-S-MD-30-60C	8.37	9.05	20.54	23.43	13.54	5.49	0.28	NA	0.23	NA	15.60	16.88	37.21	0.16	0.91	0.05	21.55
105	SCP21-S-MD-60-100	8.34	11.81	26.81	21.58	17.33	5.96	0.34	NA	0.26	NA	17.80	2.81	25.10	0.06	0.69	0.00	16.65
106	SCP22-S-MD-0-5CM	8.30	15.22	34.55	69.74	16.87	4.40	0.54	NA	0.13	NA	21.60	0.36	25.61	0.09	1.07	0.50	17.68
107	SCP22-S-MD-5-10CM	8.28	15.90	36.09	66.58	30.95	5.99	0.70	NA	0.16	NA	21.80	0.25	24.12	0.05	1.13	0.47	15.52
108	SCP22-S-MD-10-30C	8.34	14.21	32.27	46.13	37.70	6.14	0.42	NA	0.23	NA	22.20	0.43	22.67	0.08	1.07	0.47	31.47
109	SCP22-S-MD-30-60C	8.48	6.70	15.21	16.75	16.07	9.00	0.20	NA	0.27	NA	20.40	9.94	41.33	0.55	0.87	0.35	12.96
110	SCP22-S-MD-60-10C	8.60	5.60	12.72	23.26	13.08	11.72	0.20	NA	0.34	NA	21.20	20.17	57.85	0.79	0.73	0.23	13.95
111	SCP23-S-MD-0-5CM	8.37	16.28	36.96	54.67	30.79	5.35	0.63	NA	0.15	NA	22.40	0.63	21.63	0.09	1.50	0.79	14.69
112	SCP23-S-MD-5-10CM	8.38	15.78	35.82	51.81	19.15	5.22	0.54	NA	0.17	NA	15.00	0.57	33.61	0.07	1.26	0.74	28.36
113	SCP23-S-MD-10-30C	8.40	13.38	30.37	33.77	32.81	7.90	0.49	NA	0.26	NA	21.20	0.51	24.36	0.05	0.67	0.62	31.18
114	SCP23-S-MD-30-60C	8.44	8.58	19.47	14.81	15.34	11.16	0.42	NA	0.37	NA	21.00	5.03	51.59	0.11	0.42	0.30	15.27
115	SCP23-S-MD-60-10C	8.38	7.65	17.37	24.59	11.60	12.57	0.38	NA	0.41	NA	19.60	37.42	74.67	0.92	0.89	0.23	17.53
116	SCP24-S-MD-0-5CM	8.39	14.49	32.91	55.28	18.46	8.27	0.67	NA	0.42	NA	23.60	3.56	33.42	0.22	1.83	0.77	18.85
117	SCP24-S-MD-5-10CM	8.39	15.28	34.70	53.06	19.53	8.35	0.72	NA	0.29	NA	22.60	2.20	33.78	0.15	1.75	0.78	37.81
118	SCP24-S-MD-10-30C	8.31	16.14	36.65	52.40	18.12	6.60	0.53	NA	0.24	NA	22.20	3.38	36.82	0.20	1.90	0.73	24.27
119	SCP24-S-MD-30-60C	8.45	11.70	26.56	26.65	17.40	10.62	0.49	NA	0.40	NA	21.60	11.62	49.28	0.40	1.28	0.53	30.87
120	SCP24-S-MD-60-10C	8.40	8.33	18.90	14.34	9.72	10.81	0.41	NA	0.60	NA	19.00	59.93	107.65	0.83	0.81	0.25	38.86

Appendix 2

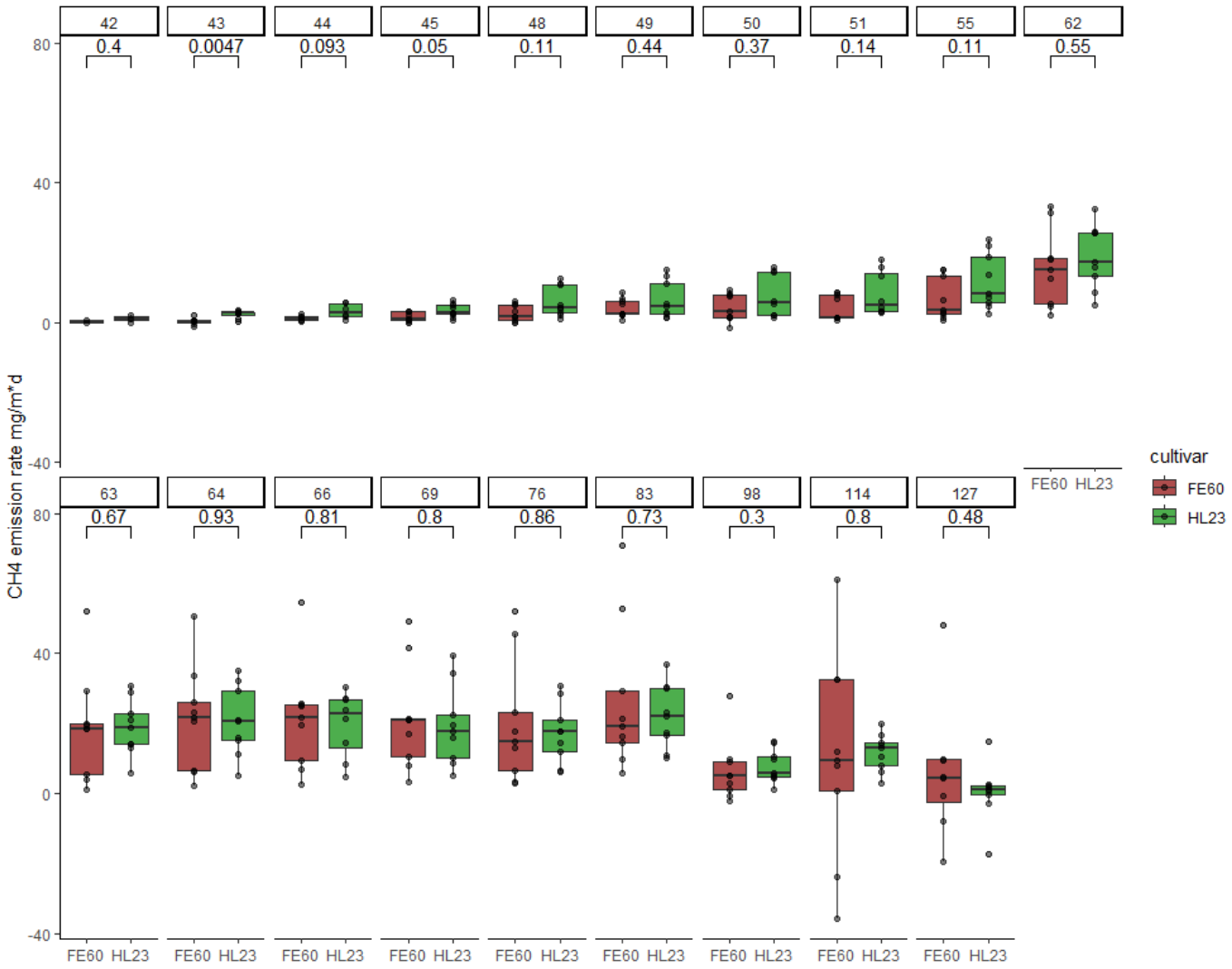

Fig. 19. Average daily methane emissions of each rice cultivar in each of the three sampling intervals (42-55, 62-76, and 83-127 days after sowing)

Appendix 3

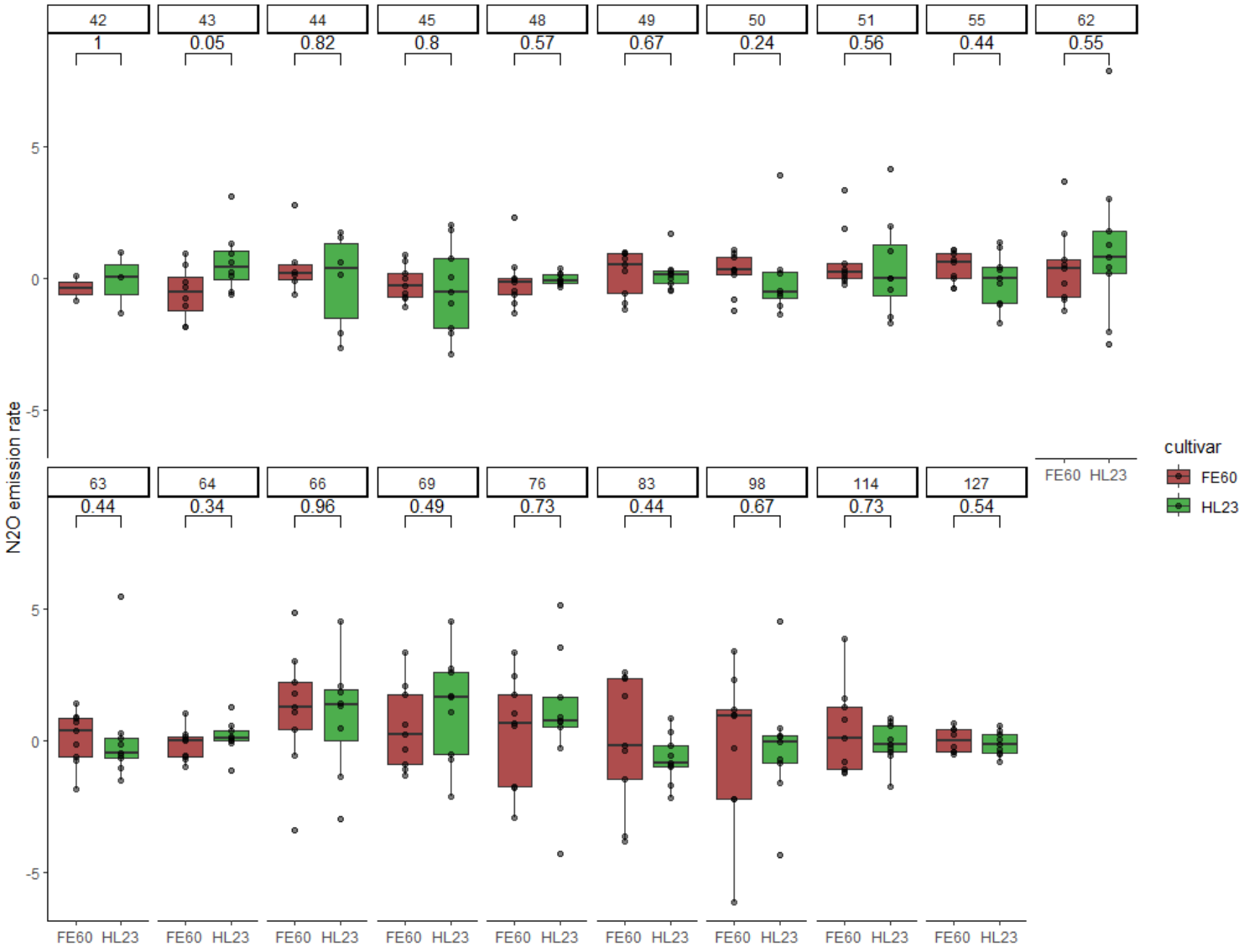

Fig. 20. Average daily nitrous oxide emissions of each rice cultivar in each of the three sampling intervals (42-55, 62-76, and 83-127 days after sowing)

Appendix 4

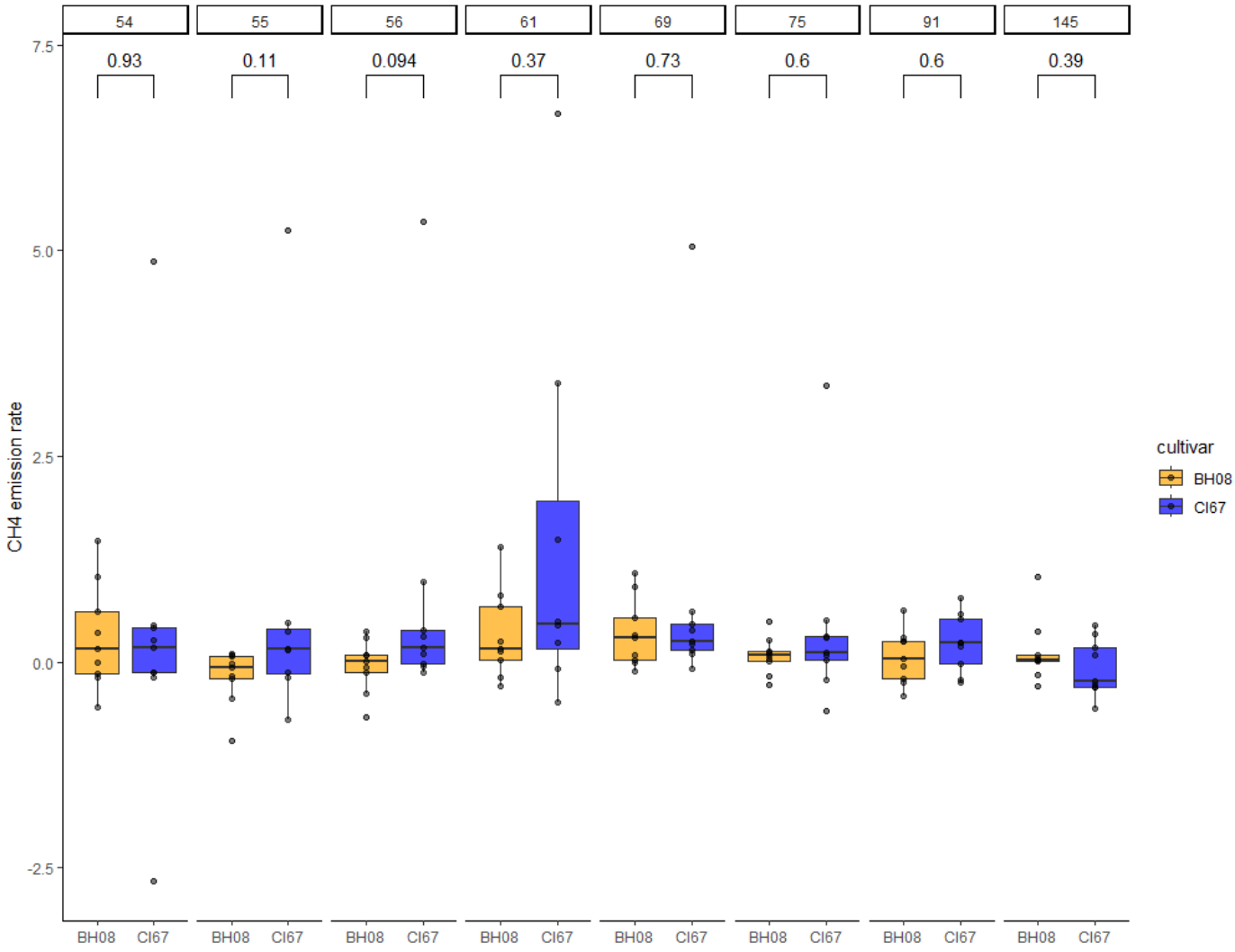

Fig. 21. Average daily methane emissions of each koronivia grass cultivar in both of the two sampling intervals (54-61 and 69-145 days after planting in field)

Appendix 5

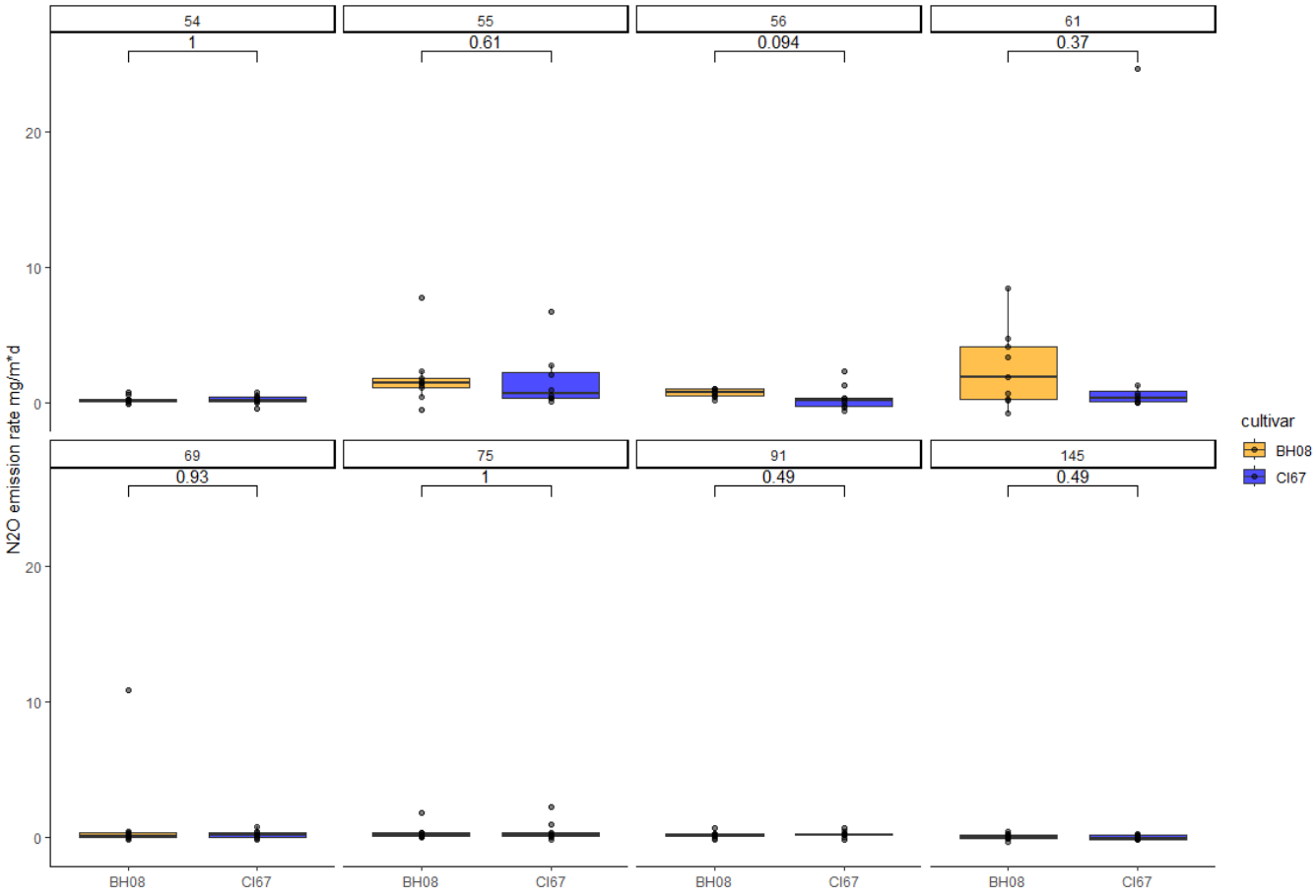

Fig. 22. Average daily nitrous oxide emissions of each koronivia grass cultivar in both of the two sampling intervals (54-61 and 69-145 days after planting in field)

Publishing and archiving

Approved students' theses at SLU are published electronically. As a student, you have the copyright to your own work and need to approve the electronic publishing. If you check the box for **YES**, the full text (pdf file) and metadata will be visible

and searchable online. If you check the box for **NO**, only the metadata and the abstract will be visible and searchable online. Nevertheless, when the document is uploaded it will still be archived as a digital file. If you are more than one author, the checked box will be applied to all authors. You will find a link to SLU's publishing agreement here:

- https://libanswers.slu.se/en/faq/228318.

☒ YES, I/we hereby give permission to publish the present thesis in accordance with the SLU agreement regarding the transfer of the right to publish a work.

☐ NO, I/we do not give permission to publish the present work. The work will still be archived and its metadata and abstract will be visible and searchable.